FINITE ELEMENT ANALYSIS OF RAFT FOUNDATION IN SOILS WITH LOW BEARING CAPACITY

BY

OJETUNDE, Isaiah Abolade

MEng/SEET/2017/6966

DEPARTMENT OF CIVIL ENGINEERING

FEDERAL UNIVERSITY OF TECHNOLOGY, MINNA

AUGUST, 2021

ABSTRACT

Load-bearing response of Raft or mat footing is affected by symmetry, load concentration and textural composition of the underlying or surrounding soil. This work presents Finite Element Analysis of raft foundation on expansive clay. Plaxis 3D computer software was used for the analysis. The result was compared with the classical Mohr-Coulomb analysis. The free swell index (*FSI*) of test clay samples collected from 0 – 1.5 metres depth ranged from 105.95 to 118.18%, which classified it under highly expansive clay. The deformation of model raft foundations were estimated at three stages namely; the initial stage, the excavation stage and the loading stage. The results revealed that the deformation of raft footing was higher at the excavation stage with a value of 4.55 $x10^{-3}$m, when compared with $615.15*10^{-6}$m recorded at the initial stage under the same load. With the introduction of model raft, the total deformation of the footing at this critical stage (excavation) reduced to 606.95 $x10^{-6}$m. Under the same threshold pressure and load-factor difference, the deformation obtained using the classical Mohr-Coulomb model is 18.442 $x10^{-3}$m, which is higher than the $601.01*10^{-6}$m obtained using the finite element analysis. Finally, the loading rate efficiency of modelled raft foundation using Finite Element Analysis is 10.3% higher than that of Classical Mohr-Coulomb model. Raft foundation analyzed using Finite Element Analysis is therefore recommended especially where the underlying strata is or has similar properties as that of expansive clay.

TABLE OF CONTENTS

Contents		**Page**
Title page		ii
Declaration		iii
Certification		iv
Dedication		v
Acknowledgement		vi
Abstract		vii
Table of Contents		viii
List of Tables		xii
List of Figures		xiii
List of Plate		xiv
List of Appendices		xv
Abbreviations, Glossaries and Symbols		xvi
CHAPTER ONE		
1.0	**INTRODUCTION**	**1**
1.1	Background to the Study	1
1.2	Statement of the Research Problem	2
1.3	Aim and Objectives of the Study	3
1.4	Scope of the Study	3
1.5	Justification of the Study	4

CHAPTER TWO

2.0	**LITERATURE REVIEW**	**5**
2.1	Finite Element Modelling	5
2.2	Raft Foundation	6
2.2.1	Need for raft foundations	6
2.2.2	Types of Raft Foundations	7
2.3	Clays and Clay Minerals	8
2.3.1	Expansive clay soil	9
2.4	Finite Element Models in Geotechnical Engineering	11
2.4.1	Mohr-Coulomb model	11
2.4.1.1.	Determination of Mohr – Coulomb criterion parameters	12
2.4.2	Nova model	12
2.4.2.1.	Determination of Nova criterion parameters	15
2.4.3	Vermeer model	16
2.4.3.1.	Determination of Vermeer model parameters	20
2.5	Foundation Modelling	21
2.5.1	Modelling of shallow foundation	21
2.5.2.	Modelling of Pile-Raft Foundation	22

CHAPTER THREE

3.0. RESEARCH METHODOLOGY 26

3.1. Materials 26

3.1.1 Soil 26

3.1.2 Plaxis 3D software 26

3.2 Methodology 26

3.2.1 Natural moisture content 26

3.2.2 Specific gravities 27

3.2.3 Sieve analysis 28

3.2.4 Atterberg limits tests 28

3.2.4.1 Liquid limit (LL) 28

3.2.4.2 Plastic limit (PL) 29

3.2.5 Compaction characteristics 30

3.2.6 Free Swell Index of soil 30

3.2.7 Consolidated Undrained Triaxial test (CU) 31

3.3 Model Raft Foundation Analysis 31

CHAPTER FOUR

4.0 RESULTS AND DISCUSSION 33

4.1 Index Properties of the soils 33

4.2 Natural Moisture Content 33

4.3 Specific Gravity of Soil Sample 33

4.4 Atterberg Limit Test 34

4.5 Compaction Characteristics 34

4.6 Free Swell Index of Test Samples 34

4.7 Consolidated Undrained Triaxial Test (CU) 35

4.8 Deformation of Samples 39

4.8.1 Initial Stage Deformation 39

4.8.2 Excavation Stage Deformation 40

4.8.3 Final Stage Deformation 41

CHAPTER FIVE

5.0 CONCLUSION AND RECOMMENDATIONS 43

5.1 Conclusion 43

5.2 Recommendation 43

5.3. Contribution to Knowledge 43

REFERENCES 44

APPENDICES 50

LIST OF TABLES

Table	Title	Page
2.1: Yield surface and plastic potential expressions function of stress state (Popa and Batali, 2010)		14
4.1: Triaxial test results of samples at depth of 0m		35
4.2: Principal stresses of test samples at 0m		35
4.3: Triaxial test results of sample at 1.0m		36
4.4: Principal stresses for sample at 1.0m depth		36
4.5: Triaxial test results of sample at 1.5m depth		37
4.6: Table from computation of the results		37
4.7: Summary of properties of test clay		38
4.8: Initial stage deformation at loaded points		39
4.9: Excavation stage deformation at loaded points		41
4.10: Final stage deformation at loaded points		41

LIST OF FIGURES

Figure	Title	Page
2.1.	Axial symmetric triaxial compression test modelled using Mohr-Coulomnb criterium	11
2.2.	c and ϕ parameters of soil	13
2.3:	Yield surface (a) and plastic potential (b) for Nova criterion	15
2.4:	Volumetric yield surface	20
3.1:	Loading points of modelled raft footing	32
4.1:	Mohr circle diagram of sample at 0 m	36
4.2:	Mohr circle diagram of sample at 1.0m depth	37
4.3:	Mohr circle diagram of sample at 1.5m depth	38
4.4:	Initial stage deformation of the soil	39
4.5:	Initial stage deformation curves of loaded points	40
4.6:	Excavation stage deformation of the soil	40
4.7:	Excavation stage deformation curve of loaded points	41
4.8:	Final stage deformation of the soil	42
4.9:	Final stage deformation curve of loaded points	42

LIST OF PLATES

Plates	Title	Page
1: Consolidated undrained test of samples		31

LIST OF APPENDICES

Appendices	Title	Page
A.	Sieve Analysis Results of Samples	50
B.	Natural Moisture Content of Samples	53
C.	Specific Gravity of Soil Samples	54
D.	Atterberg Limits of Soil Samples	55
E.	Compaction Characteristics of Soil Samples	58
F.	Free Swell Index of Soil Samples	64

ABBREVIATIONS, GLOSSARIES AND SYMBOLS

BS	British Standard
CL	clayey soil
FUTMINNA	Federal University of Technology, Minna
Gs	specific gravity
LL	liquid Limit
M	mass
m	meter
NMC	natural moisture content
NP	Non-Plastic
PI	plasticity Index
PL	plastic Limit
MDD	maximum dry density
OMC	Optimum moisture content

CHAPTER ONE

1.0 INTRODUCTION

1.1 Background to the Study

Raft foundation are sometimes referred to as raft footings (Jawad, 1998). They are formed by reinforced concrete slabs of uniform thickness that cover a wide area, often the entire footprint of the building (Jawad, 1998). Raft foundation are widely used in supporting structures for many reasons such as weak soil conditions or heavy column loads (Pusadkar and Bhatkar, 2013).

Clays are the finest grained soils. The upper limit on grain size is 0.002mm, but most of the clay particles will even be smaller (Johnson, 1969). Clay soil pose a great hazard in regions with pronounced wet and dry seasons. The annual cycle of wetting and drying causes clay soil to shrink and swell each year (Yenes *et al*., 2012)

Foundation failures are rare unless the building is located on expansive soils (Subramanian, 2009). According to Rogers *et al*., (1985), the most obvious way in which expansive soils can damage foundations is by uplift as they swell with moisture increases. Moreover, Al-Ansari (2017) deduced that raft foundation fails when its resistance is less than the action caused by the applied load. The failure of foundation of any structure tends to the failure of the entire structure which is accompanied with loss of life and as well as other economy related problems.

According to Srivastava *et al*., (2012), the causes of foundation failure include; lateral loading, construction error, unequal support, water level fluctuation, earthquake, landslide and inadequate geotechnical investigation. This foundation failure has led to building collapse of many buildings.

Numerical analysis using finite element analysis is popular in recent years in the field of foundation engineering (Mardia, 2014). To date, a variety of finite element computer programs have been developed with a number of useful facilities to suit different needs. The behaviour of soil is also incorporated with appropriate stress – strain laws as applied to discrete elements. The finite element method provides a valuable analytical tool for the analysis and design of foundations. Therefore, numerical methods such as finite element method (FEM) can be used to gain an understanding of the failure mechanisms experienced by raft foundation on expansive clay soil.

In this work, finite element model (FEM) was used to simulate the results gotten from failure of raft foundation in expansive clay soil; this model will be used in future work to evaluate the performance of a raft foundation. In addition, knowledge gained in the work will help in reducing the rate of foundation failure in such soils.

1.2 Statement of the Research Problem

Low bearing capacity soils pose problems to civil engineers in general and to geotechnical engineers in particular (Chen, 1988). Expansive soils are highly plastic soils that contain a large number of clays and are very sensitive to changes in water content.

The problems associated with low bearing capacity soils are related to bearing capacity and cracking, breaking up of pavements, and other building foundation problems (Ameta *et al*., 2007). Cracked foundations, pavements, floors and basement walls are typical types of damage done by swelling soils. Every year they cause damages requiring huge sum to maintain or repair (Wang, 2016).

The most obvious way in which expansive soils can damage foundations is by uplift as they swell with moisture increases. Swelling soils lift up and crack lightly-loaded, continuous strip footings, and frequently cause distress in floor slabs (Das and Roy, 2014)

1.3 Aim and Objectives of the Study

The aim of this work is to analysis raft foundation in soils with low bearing capacity.

The objectives of this work were:

i. determination of the physical properties of clay samples.
ii. determination the raft-soil failure pattern in soils with low bearing capacity under compressive loading.
iii. development of a model for estimating failure of raft foundation in soils with low bearing capacity.

1.4 Scope of the Study

In this work finite difference was used as a tool for the determination of the failure of raft foundation in clay soil and how it can be prevented.

Engineering tests was carried out on the soil and this include compaction test (to determine maximum dry density and optimum moisture content) and triaxial test (to find the cohesion (c) and angle of internal friction (ϕ) of the soil). The routine laboratory tests such as grain size distribution and Atterberg's limits was conducted on the disturbed samples collected.

To accomplish the modelling work the finite element package Plaxis 3D was utilized. The soil was modelled using the Mohr-Coulomb constitutive law for the model.

1.5 Justification of the Study

With the recent increase in building collapse in many parts of Nigeria, which has led to loss of lives and properties, which on many occasions have been attributed to either structural, construction or member failure including foundation. To this end a model has been developed that predicts the performance of raft foundation in soils with low bearing capacity.

CHAPTER TWO

2.0 LITERATURE REVIEW

2.1 Finite Element Modelling

The finite element method (FEM) is a numerical technique for solving problems which are described by partial differential equations or can be formulated as functional minimization (Hutton, 2004). A domain of interest is represented as an assembly of finite elements**.** Approximating functions in finite elements are determined in terms of nodal values of a physical field which is sought.

Finite element procedures are widely used in engineering analysis presently (Kraskiewicz *et al.,* 2015*),* and its use is expected to increase significantly in years to come. The procedures are employed extensively in the analysis of solids and structures (De-Weck and Kim, 2004) and of heat transfer and fluids, and indeed, finite element methods are useful in virtually every field of engineering analysis.

As is often the case with original developments, it is rather difficult to quote an exact "date of invention," but the roots of the finite element method can be traced back to three separate research groups: applied mathematicians (Courant, 1943); physicists (Synge, 1957); and engineers (Argyris 1965). Although in principle published already, the finite element method obtained its real impetus from the developments of engineers. The original contributions appeared in the papers by Argyris and Kelsey (1955); Turner *et al*., (1956); and Clough (1960). The name "finite element" was coined in the paper Clough (1960).

Important early contributions were those of Argyris (1965) and Zienkiewicz and Cheung (1967). Since the early 1960s, a large amount of research has been devoted to

the technique, and a very large number of publications on the finite element method is available. A continuous physical problem is transformed into a discretized finite element problem with unknown nodal values. For a linear problem a system of linear algebraic equations should be solved. Values inside finite elements can be recovered using nodal values.

2.2 Raft Foundation

Raft or mat foundation is a combined footing that covers the entire area beneath a structure and supports all walls and columns (Garba, 2014). The raft or mat normally rests directly on soil or rock, but can also be supported on piles as well. A raft is used when loads are large and pad foundations give excessive settlements. Total and differential settlements usually govern the design. A detailed structural design is necessary which provides slab thickness and reinforcement to resist bending and shear.

2.2.1 Need for raft foundations

Gupta (2007) outlined that raft foundation is generally suggested in the following situations:

1. Whenever building loads are so heavy or the allowable pressure on soil so small that individual footings would cover more than floor area.
2. Whenever soil contains compressible lenses or the soil is sufficiently erratic and it is difficult to define and assess the extent of each of the weak pockets or cavities and thus estimate the overall and differential settlement.
3. When structures and equipment to be supported are very sensitive to differential settlement.

4. Where structures naturally lend themselves for the use of raft foundation such as silos, chimneys, water towers.
5. Floating foundation cases wherein soil is having very poor bearing capacity and the weight of the super-structure is proposed to be balanced by the weight of the soil removed.
6. Buildings where basements are to be provided or pits located below ground water table.
7. Buildings where individual foundation, if provided, will be subjected to large widely varying bending moments which may result in differential rotation and differential settlement of individual footings causing distress in the building.

In case of soils having low bearing pressure, Gupta (2007) also outlined three advantages of using a raft foundation:

a. Ultimate bearing capacity increases with increasing width of the foundation bringing deeper soil layers into the effective zone.
b. Settlement decreases with increased depth.
c. Raft foundation equalises the differential settlement and bridges over the cavities

2.2.2 Types of raft foundations

Gupta (2007) classified raft foundation into various types on the following basis:

1. Based on the method of their support, raft can be:
    a. Raft supported on soil,
    b. Raft supported on piles
    c. Buoyancy raft.

2. On the basis of structural system adopted for the structure of the raft, these can be classified as:
    a. Plain slab rafts, which are flat concrete slabs, having a uniform thickness throughout. This can be with pedestals or without pedestals.
    b. Beam and slab raft which can be designed with down stand beam or up stand beam systems.
    c. Cellular raft or framed raft with foundation slab, walls, columns and one of the floor slabs acting together to give a very rigid structure.

2.3 Clays and Clay Minerals

First, the basic terms concerning clays and clay minerals must be defined. A clay soil is any fine-ground, natural, earthy argillaceous material (Grim, 1962). This, however, is a rock term, and not in term of particle size. The term “clay” has no generic significance because it is used for residual weathering products, hydrothermally altered products and sedimentary products. As a particle size term, the size fraction comprised of the smallest particles is called clay fraction. The Wenworth scale defines the clay grade as finer than 2μm (Wenworth, 1922); which is used by many engineers and scientists.

Clays and clay minerals are very important industrial minerals. There are several documented industrial applications of clay minerals. Clay is an abundant raw material which has an amazing variety of uses and properties that are largely dependent on their mineral structures and composition, though there may be other factors which are important in determining the properties and application of clays (Grim, 1950).

Clay is a fine-grained soil that combines one or more clay minerals with traces of metal oxides and organic matter. Geologic clay deposits are mostly composed of phyllosilicate minerals containing variable amounts of water trapped in the mineral structure (Guggenheim *et al.*, 1995). Clays vary in plasticity, all being more or less malleable and capable of being moulded into any form when moistened with water. The plastic clays are used for making pottery of all kinds, bricks and tiles, tobacco pipes, firebricks, and other products.

Clays are distinguished from other fine-grained soils by differences in size and mineralogy. Silts, which are fine-grained soils that do not include clay minerals, tend to have larger particle sizes than clays, but there is some overlap in both particle size and other physical properties, and there are many naturally occurring deposits which include silts and also clay. The distinction between silt and clay varies by discipline. Geologists and soil scientists usually consider the separation to occur at a particle size of 2μm (clays being finer than silts), sedimentologists often use 4-5 μm, and colloid chemists use 1μm (Guggenheim *et al.,* 1995). Geotechnical Engineers distinguish between silts and clays based on the plasticity properties of the soil, as measured by the soils' Atterberg limits. ISO 14688 grades clay particles as being smaller than 2μm and silts larger.

2.3.1 Expansive clay soil

Expansive soils pose a severe threat to civil engineering infrastructure worldwide (Guney *et al.,* 2007). Excessive cost of damages to infrastructure mainly due to expansive soils is reported each year (Mughieda and Hazirbaba, 2015). Expansive clay soils are found in many parts of the world (Guney *et al.*, 2007). These soils are highly heterogeneous and unpredictable given their volume change cycle of swelling

and shrinkage occasioned by environmental and seasonal variations (Dang *et al.,* 2016).

Damages of structures caused by expansive soils have been reported from different locations in the clay plain (Lates *et al*., 1983). The damages include buildings, roads, factories and hydraulic structures and were attributed to lack of proper identification and classification of expansive soils and improper design of the foundations of the damaged structures.

For the purpose of foundation design, it is very imperative to carefully recognize and evaluate the expansive soil's capacity to swell or expand (Samtani and Nowatzki, 2006) so as to forestall the risk of potential structural failure and resultant economic losses (Sarkar and Islam, 2012). The capacity to swell depends on the mineral content of the soil fines or quantity of monovalent cations absorbed on the surface of the clay minerals (Dang *et al.*, 2016). Montmorillonite clays tend to exhibits very high degree of swelling as compared to Illite and Kaolinite which both have moderate to none swell potentials (Samtani, and Nowatzki, 2006).

Expansive soils that exhibit swelling problems consist of silty mudstones, bentonitic mudstones, argillaceous limestone, marls and altered conglomerates (Al-Rawas *et al.*, 2005). Other factors that affect the expansive soil's ability to swell are its relative density, moisture content at compaction, permeability, dry density, location of the groundwater table, past and existing overburden pressure, presence of vegetation and trees (Khemissa and Mahamedi, 2014).

2.4 Finite Element Models in Geotechnical Engineering

2.4.1 Mohr-Coulomb model

Coulomb proposed the first plasticity model in soil mechanics. It is composed of two symmetrical lines in Mohr's plane (σ, τ), having an angle ϕ with the normal stresses' axis, σ and having as equation:

$$F(\sigma_{ij}) = \sigma_1 - \sigma_3 - (\sigma_1 + \sigma_3)\sin\emptyset - 2c\cos\emptyset \leq 0 \quad (2.1)$$

Where:

σ_1 and σ_3 are the extreme main stresses.

Parameter c represents the soil cohesion,

while ϕ is the internal friction angle.

In the space of main stresses (σ_1, σ_2, σ_3) the surface defined by function F is a pyramid with hexagonal section having as axis the line $\sigma_1 = \sigma_2 = \sigma_3$.

The plastic potential defined as a function of the extreme main stresses is:

$$G(\sigma_{ij}) = \sigma_1 - \sigma_3 + (\sigma_1 + \sigma_3)\sin\varphi + \text{const} \quad (2.2)$$

Where:

φ is the dilatancy angle (φ = ϕ if it is an associated criterion).

The elasticity associated to the Mohr – Coulomb criterion is a linear Isotropic-Hooke type one. The criterion contains 5 mechanical parameters:

i. E – elasticity modulus,
ii. ν - Poisson's coefficient: elastic parameters;

iii. c, ϕ, ψ: plastic parameters.

2.4.1.1. Determination of Mohr – Coulomb criterion parameters

The parameters of the Mohr-Coulomb criterion can be determined using a triaxial compression, axial symmetric laboratory test. Figure 1 presents the results of such a test and the manner in which the parameters can be determined (ε_1 – main specific strain; ε_v – volumetric strain).

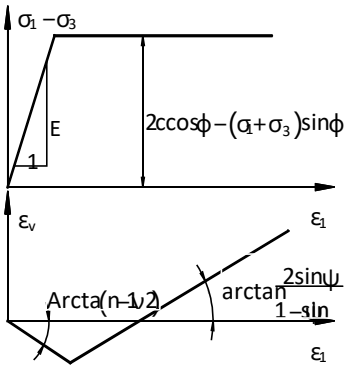

Figure 2.1: Axial symmetric triaxial compression test modelled using Mohr–Coulomb criterion

If the soil cohesion is not nil (cohesive soils), a minimum of two laboratory tests are required, conducted under different consolidation pressures, for determining the parameters ϕ and c. For each test, the axial stress at failure, σ_1 and the consolidation pressure are plotted in the $((\sigma_1 + \sigma_3)/2, (\sigma_1 - \sigma_3)/2)$ axis system. The slope of the line ($\sin\phi$) provides the ϕ value, while the ordinate for x = 0 ($c \cos\phi$) gives the c value (Figure 2.2).

2.4.2 Nova model

Nova model (1982), is an elasto–plastic with isotropic plastic hardening criterion, inspired by the Cam-clay model but adapted to sand behaviour, Figure 2.2.

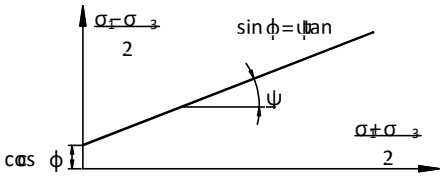

Figure 2.2: c and ϕ parameters of soil

It has been developed based on tests conducted on cylindrical sand samples, which explains the formulation as a function of stress invariants, p (mean pressure) and q (deviatoric stress) and plastic strain invariants, ε_v^p (plastic volumetric strain) and ε_v^p (plastic deviatoric strain).

The elastic component of the strain is linked to the stress state by the following incremental relationship:

$$d\varepsilon_{ij}^e = \mathrm{L}_o \eta_{ij} + B_o \frac{dp}{3p} \delta_{ij} \tag{2.3}$$

Where:

L_o and B_o are two specific parameters of the model

$\eta_{ij} = \frac{\sigma_{ij} - p\delta_{ij}}{p}$,

$p\delta_{ij}$ is Kroneker's tensor)

The mean pressure, p and the deviatoric stress, q are calculated using the following formulas:

$$p = \frac{\sigma_1 + \sigma_2 + \sigma_3}{3} \tag{2.4}$$

$$q = \sqrt{\frac{(\sigma_1 - \sigma_2)^2 + (\sigma_1 - \sigma_3)^2 + (\sigma_2 - \sigma_3)^2}{2}} \tag{2.5}$$

The expressions for the yield surface and plastic potential are given in Table 2.1.

Table 2.1: Yield surface and plastic potential expressions function of stress state (Popa and Batali, 2010)

Stress state	Stress-dilatancy relationship	Yield surface F (p, q, p_c) and plastic potential G (p, q, p_c)
$\frac{q}{p} \leq \frac{M}{2}$	$\frac{d\varepsilon_v^p}{d\varepsilon_d^p} = \frac{M^2}{4\mu}\frac{p}{q}$	$F(p,q,p_c) = G(p,q,p_c)$ $G(p,q,p_c) = \frac{4\mu}{M^2} - \frac{q^2}{p^2} + 1 - \frac{p_c^2}{p^2}$
$\frac{q}{p} \geq \frac{M}{2}$	$\frac{d\varepsilon_v^p}{d\varepsilon_d^p} = \frac{M^2}{\mu} - \frac{p}{\mu q}$	$F(p,q,p_c) = \frac{q}{p} - \frac{M}{2} + min\left(\sqrt{1+\mu}\frac{p}{p_c}\right) = 0$ $G(p,q,p_c) = \frac{q}{p} - \frac{M}{1-\mu}\left[1 - \mu\left(\frac{p}{p_{co}}\right)^{\frac{1-\mu}{\mu}}\right] = 0$

Variables p_{co} and p_c correspond to the intersection of the plastic potential with the isotropic compression axis for $\frac{q}{p} \geq \frac{M}{2}$ and to the variable characterizing the hardening, respectively. p_c is function of the plastic strain invariants:

$$p_c = p_{co} exp\left[\frac{\varepsilon_v^p + D\varepsilon_d^p}{1 - B_o}\right] \tag{2.6}$$

where:

$$\varepsilon_v^p = \varepsilon_1^p + \varepsilon_2^p + \varepsilon_3^p \tag{2.7}$$

$$\varepsilon_d^p = \sqrt{\frac{\left(\varepsilon_1^p - \varepsilon_2^p\right)^2 + \left(\varepsilon_1^p - \varepsilon_3^p\right)^2 + \left(\varepsilon_2^p - \varepsilon_3^p\right)^2}{2}} \tag{2.8}$$

2.4.2.1. Determination of Nova criterion parameters

Nova criterion is described by eight parameters determined based on triaxial axial symmetric compression tests, in drained conditions, with one unloading – reloading cycle, Figure 2.3. (Mesta, 1993).

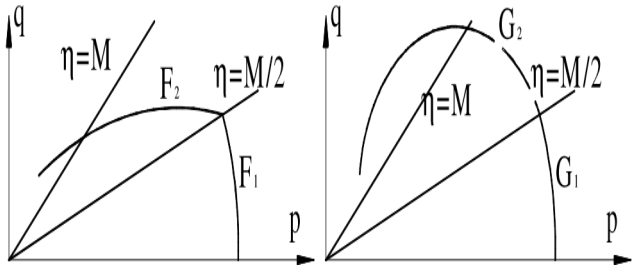

a b

Figure 2.3: Yield surface (a) and plastic potential (b) for Nova criterion

i. **B_o**: elastic behaviour parameter determined by the points on the unloading curve. These points form a line in the (ε_v^p, lnp) plan; the slope of this line provides B_o value.

ii. **L_o**: elastic behaviour parameter determined by the points on the unloading curve. These points form a line in (ε_d^e , q/p) plan, which slope gives L_o value.

iii. **l**: parameter linked to the initial tangent to the behaviour curve

$$(\varepsilon_1, q): \frac{dq}{d\varepsilon_1}(\sigma_1 = \sigma_3) = \frac{9\sigma_3}{6L_0+1} \tag{2.9}$$

iv. **D**: parameter modelling the dilatancy. D is the limit of $d\varepsilon_q^p / d\varepsilon_d^p$ when the failure is approaching.

v. **M**: parameter related to the extreme point of the plastic volumetric strain ($d\varepsilon_v^p = 0$). M can be determined from the $(\varepsilon_1, \varepsilon_v^p)$ graph. The strain ε_v^p is evaluated as the difference between the experimental volumetric strain (or total strain) and the elastic volumetric strain calculated using Nova criterion (B_o being known).

vi. **μ**: parameter related to the soil sample failure. It is determined using the relationship: $\mu = {(\eta_f - M)}/{D}$,

where η_f corresponds to stress rate ${q}/{p}$ at failure.

vii. **m**: parameter related to the position of the characteristic state (the extreme point of the volumetric strain, $d\varepsilon_v = 0$). Its determination is delicate and often is preferred to be adjusted successively based on an estimated value of the characteristic state. The equation of the tangent to the curve (ε_1, q) for the point $(\varepsilon_1, d\varepsilon_v = 0)$ can be written and the following relationship is deduced by equation 2.10:

$$m = \frac{-(1-B_o)(3-\eta_c)(M-\eta_c)}{\mu B_o D + 1(M-\eta_c)} \quad (2.10)$$

where η_c is the stress rate ${q}/{p}$ for the characteristic state.

viii. $\boldsymbol{p_{co}}$: parameter depending on the initial state, equal to the consolidation pressure of a triaxial test or calculated function of initial stress state so that no initial elastic domain exists into the soil mass.

2.4.3 Vermeer model

The constitutive model developed by Vermeer (Vermeer,1982), is an elasto–plastic model with two hardening mechanisms. The first hardening mechanism is a pure volumetric one (consolidation), while the second one is purely deviatoric (shear). The plastic potential coincides with the yield surface for the first mechanism (associated potential), while for the second mechanism a relationship type stress – dilatancy is used for the plastic potential. The elastic part of the criterion is non-linear isotropic and derives from a potential.

The elastic component of the Vermeer model is based on Hooke elasticity with a Young's modulus depending on the stress state and a nil Poisson's coefficient. The relationship linking stresses and strains is expressed in equations 2.11 to equation 2.22:

$$\sigma_{ij} = 2\varepsilon_{ij}G_s(\sigma_{ij}) \tag{2.11}$$

With

$$G_s(\sigma_{ij}) = G_o[\,{}^{\sigma_n}/_{p_o}\,]^{(1-\beta)} \tag{2.12}$$

where:

p_o is an initial isotropic reference pressure for which the volumetric strain is $\varepsilon_o^e(2G_O\varepsilon_o^e = 3p_0)$,

β is a constant

σ_n represents the following stress invariant:

$$\sigma_n^2 = \frac{\sigma_1^2+\sigma_2^2+\sigma_3^2}{3} \tag{2.13}$$

The volumetric yield surface has the following expression:

$$F_v\left(\sigma_{ij}, \varepsilon_{ij}^p\right) = G_v\left(\sigma_{ij}, \varepsilon_{ij}^p\right) = \varepsilon_o^c[\,{}^{\sigma_n}/_{p_o}\,]^{\beta} - \varepsilon_{vc}^p \tag{2.14}$$

Where:

ε_o^c is a constant and

ε_{vc}^p represents the hardening parameter of the yield surface.

The deviatoric yield surface has the following expression:

$$F_c\left(\sigma_{ij}, \varepsilon_{ij}^{p}\right) = -3pII_2 + III_3 A(x) = 0 \quad (2.15)$$

Where:

p, II_2, III_3 are the classical invariants using the sign convention of the continuum medium mechanics:

$$p = {-(\sigma_1+\sigma_2+\sigma_3)}/{3} \quad (2.16)$$

$$II_2 = -\sigma_1\sigma_2 - \sigma_1\sigma_3 - \sigma_2\sigma_3 \quad (2.17)$$

$$III_3 = -\sigma_1\sigma_2\sigma_3 \quad (2.18)$$

A(x) is a scalar function defined as follows:

$$A(x) = \frac{27[3+h(x)]}{[2h(x)+3][3-h(x)]} \quad (2.19)$$

$$c = \frac{6\sin\emptyset_p}{3-\sin\emptyset_p} \quad (2.20)$$

$$h(x) = \sqrt{{x^2}/{4} + cx} - {x}/{2} \quad (2.21)$$

$$x = \gamma^p 2G_o {[{p_o}/{\sigma_n}]^{\beta}}/{p_o} \quad (2.22)$$

where c is a parameter defined function of the maximum internal friction angle $\emptyset_p$ and γ^p represents the plastic distortion: $\gamma^p = \left[{e_{ij}^p e_{ij}^p}/{2}\right]^{0.5}$

These complex expressions cover a very simple reality. In fact, the deviatoric yield surface was built so that it is reduced to Drucker-Prager, (Mestat, 1993), criterion when the conditions of a triaxial axial symmetric test conditions are fulfilled. In this case the yield surface equation is reduced to the simple relationship in equations 2.23 to equations 2.27:

$$F_c = {}^{q}/_{p} - h(x) = 0 \tag{2.23}$$

The plastic potential is not associated and it is built using the following relationship:

$$G_c(\sigma_{ij}) = \sqrt{{}^{2s_{ij}s_{ij}}/_{3}} - 4p(\sin\varphi_m)/3 \tag{2.24}$$

By definition, angle φ_m is the dilatancy angle which is related to the stress state by the following:

$$\sin\varphi_m = \frac{\sin\emptyset_m - \sin\emptyset_{cv}}{1 - \sin\emptyset_m \sin\emptyset_{cv}} \tag{2.25}$$

Where:

$\emptyset_{cv}$ is the internal friction angle at constant volume

Angle $\emptyset_m$ is related to the stress state by:

$$\sin\emptyset_m = \frac{\sqrt{9 - A(x)}}{1 - A(x)} = \frac{3q}{6p + q} \tag{2.26}$$

Failure for Vermeer model is obtained for the following stress rate $(q/p)_r$

$$(q/p)_r = \frac{\sin\emptyset_p}{3 - \sin\emptyset_p} \tag{2.27}$$

Thus, Vermeer model has six parameters: ε_o^e, ε_o^c, $\emptyset_p$, $\emptyset_{cv}$, β, and p_o, . The reduced number of parameters represents an important advantage in using this constitutive law. Figure 2.4 presents the volumetric and the deviatoric yield surfaces for Vermeer model.

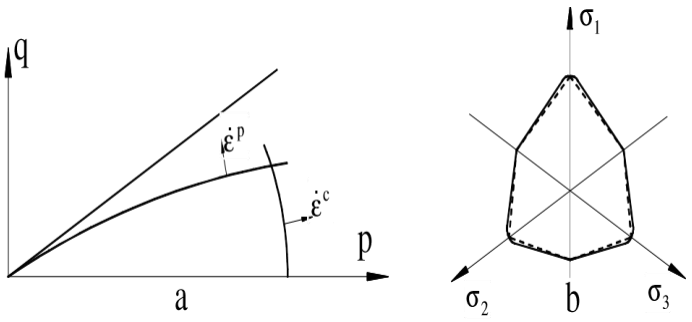

Figure. 2.4: Volumetric yield surface (a) and deviatoric yield surface (b) for Vermeer model

2.4.3.1 Determination of Vermeer model parameters

As for Nova criterion, the parameters of Vermeer model are determined based on triaxial compression, axial symmetric tests, in drained conditions and with one unloading–reloading cycle, (Mestat, 1990).

i. $\boldsymbol{\varepsilon_o^e}$ **and** $\boldsymbol{\beta}$: elastic behaviour parameters determined for the unloading curve. These points form a line on the $(\ln\varepsilon_n^e, \ln\sigma_n)$ graph. The equation of this line is presented in equations 2.28 to equations 2.31:

$$\ln\varepsilon_n^e = \beta\ln\left({}^{p_o}/_{\sigma_n}\right) + \ln\left({}^{\varepsilon_o^e}/_{3}\right) \tag{2.28}$$

with $\varepsilon_n^e = \left[{}^{e_{ij}^e e_{ij}^e}/_{2}\right]^{0.5}$ and $\sigma_n = \left({}^{\sigma_{ij}\sigma_{ij}}/_{3}\right)^{0.5}$

ii. $\boldsymbol{\varepsilon_o^c}$: parameter related to the initial tangent to the graph

$$(\varepsilon_1, q), \frac{d_q}{d\varepsilon_1}(\sigma_1 = \sigma_3) = \frac{9\sigma_3}{\varepsilon_o^e(2+\beta)+\varepsilon_0^c\beta} \tag{2.29}$$

iii. $\emptyset_p$ parameter related to the soil sample failure; $\emptyset_p$ is the maximum friction angle.

iv. $\emptyset_{cv}$ parameter related to dilatancy modelling. Angle $\emptyset_{cv}$ is determined using the following relationship:

$$\sin \emptyset_{cv} = \frac{\sin \emptyset_p - \sin \varphi_m}{1 - \sin \emptyset_p \sin \varphi_m} \quad (2.30)$$

with

$$\sin \varphi = \frac{3d\varepsilon_v}{4(d\varepsilon_3 - d\varepsilon_1)} \quad (2.31)$$

Where:

φ represents the dilatancy angle during the test and

φ_m is its limit before failure

v. $\boldsymbol{p_o}$ **:** parameter depending on the initial state, equal to the consolidation pressure for a triaxial compression test or calculated function of the initial state so that no initial elastic domain exists in the soil mass.

2.5 Foundation Modelling

2.5.1 Modelling of shallow foundation

Shallow foundations are the integral part of a structure that transmits the load directly to the underlying soil in shallow depths. Generally, foundations are considered to be shallow when the depth is less than approximately three metres, or less than the breadth of the footing.

When modelling a shallow foundation in the field, Johnson *et al.*, (2015) concluded that it is important to include all the major factors attributing to the footing's behaviour. The constitutive parameters, stress history and the interactions between elements are all key aspects to consider. The work done by Johnson *et al*., (2015) showed that a numerical prediction is as good as the input data placed into the model. In a controlled environment like the one created by Terzaghi and Peck (1948), numerical models can be accurate. However, in the field, randomness and uncertainty

are factors that must be accounted for and addressed. Numerical models can offer a great deal of information when used correctly, and they can provide a platform for developing design procedures for industry.

Conte *et al.* (2013) worked on the Progressive failure analysis of shallow foundations on soils with strain-softening behaviour and discovered that a finite element approach in which a non-local elasto-viscoplastic constitutive model in conjunction with the Mohr–Coulomb yield function is incorporated, has been proposed to predict the response of strip footings resting on soils with strain-softening behaviour. This behaviour is simulated by reducing the strength parameters with increasing the accumulated deviatoric plastic strain.

Johnson *et al*. (2015) verified the reliability and sensitivity of the FEM shallow foundation meshes, by comparing the load-deflection curves from the models with Terzaghi and Peck's (1948) pressure curves. In a controlled experiment Terzaghi and Peck load tested 300 mm square plates. Load-displacement curves were established for the square plates in three separate sand densities. The sand densities corresponded to a constant penetration blow counts (N) of 10, 30 and 50. Where the magnitude of the blow count represents the sand's strength (that is increased blow count gives higher stiffness)

2.5.2 Modelling of pile-raft foundation

A piled raft foundation is a composite structure with three components: subsoil, raft and pile (Al-Damluji and Al-Baghadadi, 2012). These components are related to each other through a complex soil structure interaction scheme, including the pile-soil interaction, pile-pile interaction, raft-soil interaction, and finally the pile-raft interaction.

Generally, the construction of a piled raft foundation system is similar to the current practices used to construct a pile group foundation in which a cap is normally cast directly on the ground. Although this installation of a cap will allow a significant percentage of the load to be transmitted directly from the cap to the ground, the pile group is usually designed conservatively by ignoring the bearing capacity of the raft (in this case the pile cap). The raft alone can provide an adequate bearing capacity; however, it may induce excessive settlement. Therefore, the concept of settlement reducer piles was presented by Burland *et al*. (1978`) in which the piles are used to limit the average and differential settlements.

Outstanding contributions on piled foundations and piled raft foundations were made by pioneering workers such as Berezantzev *et al*., (1961), Vesic (1972), Burland (1973), Meyerhof (1976), Semple and Rigden (1984), Poulos (1989), Fleming *et al*., (1992) among a very large number of researchers. Further, various computer softwares are now available for the study of piles and piled raft foundations and have been reported by many researchers. For example, PILEGRP (Chow, 1989), UNIPILE (Fellenius, 2004), CAPWAP (Lee *et al*., 1996) GASP (Poulos, 1991), GROUP (Reese and O'Neill, 1989), FLAC (Hewitt and Gue, 1994), NAPRA (Russo, 1998), FLAC (Small and Zhang. 2000), PLAXIS (Prakoso and Kulhawy, 2001), ANSYS (Liang *et a.l*, 2003), PRAB (Kitiyodom and Matsumoto, 2003), ABAQUS (Reul and Randolph, 2003) and among others.

Many researchers also proposed that the behaviour of raft foundation can be studied by using finite element approach. Shihada and Hamad (2008), compared results from analysis using the conventional approach and the Finite element approach (SAP2000 software). They concluded that moment value obtained from conventional method is more than the finite element method. Al-Ansari *et al.,* (2009) studied the design of

raft foundation in loose sand and found that using software results are more accurate. SaadEldin and El-Helloty (2014), analysed raft foundation using PLAXIS programme to study the effect of opening position and different types of soil. They found that opening and type of soil have important effect on settlement of soil and moment of raft foundation. Halkude *et al.* (2014), carried out dynamic analysis using response spectra. The soil flexibility is incorporated in the analysis using spring model for incorporating soil flexibility and FEM model for diserization of raft. They found that SSI significantly affects the response of the structure; FEM is effective approach for consideration of elastic continuum beneath foundation. Patil *et al.,* (2016), carried out the effect of soil flexibility on the performance of the building frame resting on raft foundation. They found that base shear increases due to SSI effect. The effect of SSI increases and tends to become prominent with increasing softness of the soil.

Alnuaim *et al*. (2013) worked on 3D modelling of piled raft foundation subjected to vertical loading and the FEM created in the study was able to simulate the results of a centrifuge test for a piled raft foundation under vertical loading and discovered that the load for each component obtained from the FEM were similar to the loads in the centrifuge model.

Oh *et al*. (2008) worked on finite element modelling for piled raft foundation in sand and series of case studies were conducted on un-piled raft and piled raft foundation in sandy subsoil condition and discovered that under the working load intensity of 215kN/m^2, maximum settlements for 0.25m thickness raft are 33mm and 44mm for the 8m×8m and 15m×15m rafts respectively and increasing the raft thickness to 3m reduced these maximum values to 31mm and 40mm respectively.

Salah *et al.* (2015) used finite element to modify Winkler model for raft foundation supported on dry granular soils and in an attempt to modify traditional Winkler model to take shear forces between adjacent soil prisms into account in computing subgrade reactions and bending moments in raft foundations, two finite element soil simulations was considered in their study and in the first model, Winkler simulation was adopted while in the second one soil mass was simulated with brick finite element.

CHAPTER THREE

3.0. RESEARCH METHODOLOGY

3.1. Materials

3.1.1 Soil: The soil used in this investigation was collected using the disturbed sampling technique at depths of 0m, 1m and 1.5m from borrow pits around Birgi Village, a suburb of Minna, Niger State, Nigeria. The soil samples were carefully packaged and transported to soil Mechanics /Geotechnics Laboratory, Federal University of Technology, Minna for detailed investigation.

3.1.2 Plaxis 3D software: The Finite element analysis of model raft foundation in clay was done by using PLAXIS 3D 2018 software depending with correlated compatibility with Mohr-Coulomb model. All the data necessary for the Mohr-Coulomb model were generated. These parameters with their standard units are listed as: E: Modulus of elasticity [kN/m^2], ϕ: Angle of internal friction [°], υ: Poisson's ratio [-], c: Cohesion [kN/m^2], ψ: Angle of dilatancy [°], γ_{sat}, γ_{unsat}: Saturated and Unsaturated unit weight respectively [kN/m^3] (Plaxis 3D 2018).

3.2. Methodology

Index properties: Natural moisture content, specific gravities, sieve analysis and Atterberg limits tests were conducted. in accordance with test procedures specified in BS 1377: 1990.

3.2.1 Natural moisture content

The procedure adopted involved weighing three empty cans to the nearest 0.01g ($M_{1)}$. Some quantity of fresh soil sample was placed in each of the cans and weighed again

to the nearest 0.01g (M_2). The cans containing the wet sample were place in an oven at 100 to 105°C to dry. The cans, containing the dried soil were weighed (M_3). The natural moisture content was then determined from:

$$NMC = \frac{M_2 - M_3}{M_3 - M_1} \quad (3.1)$$

Where:

M_1 = Mass of empty container

M_2 = Mass of container with wet soil

M_3 = Mass of container with dry soil

3.2.2 Specific gravities

Specific gravity is referred as the ratio of the density of a substance to the density of a reference substance such as water. ASTM D854 suggests a method to determine fine grained- soil specific gravity. Samples are oven-dried at 105 for a period of 16 to 24 hours. To perform the test, it is necessary to have empty weight of pycnometer and weight of pycnometer with oven dry soil. Then add water to cover the soil in the pycnometer and screw on the cap. To remove entrapped air, it is necessary to shake the pycnometer well and connect it to the vacuum pump for about 10 to 20 minutes, finally fill the pycnometer with water.

The Specific gravity of soil solids Gs is calculated using the following equation

$$Gs = \frac{W_2 - W_1}{(W_4 - W_1) - (W_3 - W_2)} \quad (3.2)$$

Where:

W1 = Empty weight of pycnometer

W2 = Weight of pycnometer + oven dry soil

W3 = Weight of pycnometer + oven dry soil + filled water

W4 = Weight of pycnometer + filled with water only

3.2.3 Sieve analysis

The procedure adopted involved soaking 300g of the dry soil for 24hr and then washing through sieves 2.0mm and 0.075mm. The washing was continued until the water from the washed soil became crystal clear. The retained samples during washing on sieve size 2.0 and 0.075mm were carefully collected and placed in a pan, which was in turn placed in oven at 105 to 110^{o}C for 24 hours. Set of sieves were measured empty and arranged sequentially with the sieve having the largest apertures on top and that with the lowest size below as follows; 5.0, 3.35, 2.0, 1.18, 0.85, 0.60, 0.425, 0.300, 0.150, and 0.075mm, and ending with the pan at the base. The oven dried samples were poured into the uppermost sieve and the set of the sieves placed on a mechanical sieve shaker, and allowed to shake for 10 minutes. The weight of each sieve with the retained soil was taken and recorded. The weights of empty sieves were subtracted to give weight of the retained soil on each sieve. The percentage of total sample passing each of the sieves was calculated.

3.2.4 Atterberg limit tests

3.2.4.1 Liquid limit (LL)

Cone penetrometer method of liquid limit determination was used. Reasonable quantity of air-dried sample was pulverized and sieved through 425μm sieve. About 200g of the sieved sample was placed on a flat glass and mixed thoroughly with clean water using spatula until the soil mass become a thick paste. The paste was pushed into the cup with spatula, making sure air was not trapped, until filled. The top of the

soil was trimmed with the top of the cut and placed beneath the cone. The cone was then lowered so that it just touched the surface of the soil. When the cone was in correct position, a slight movement of the cup gives a small mark on the surface of the soil and the reading of the dial gauge was recorded.

The cone was then released for a period of 1-5 seconds. After penetration, the dial gauge was lowered to the new position of the cone shaft and readings recorded. The difference between the readings at the beginning and at the end of the test was recorded as the cone penetration. Average of two penetrations was recorded. The cone lifted out and cleaned. A moisture content sample of about 10g was taken from the area penetrated by the cone for moisture content determination. The soil was then removed from the cup, remixed and the procedure outlined above was repeated using the same sample with more water added until penetration of about 20mm was recorded. The relationship between the moisture contents and cone penetration was plotted. From the plotted graph, moisture content at 20mm penetration was taken as liquid limit of the soil.

3.2.4.2 Plastic limit (PL)

About 20g of the pulverized soil sample, sieved through 425μm sieve was used for the test. The soil was thoroughly mixed with clean water. A small sample of soil ball like was then rolled between the hand and glass plate. The rolling continues until a thread of about 3mm in diameter was obtained, the thread crumbled at the stage. The portion of the crumbled soil was the gathered and placed in moisture can for moisture content determination. The plasticity Index (PI): is the range of water content over the soil is in the plastic condition.

$$\text{Plasticity Index (PI)} = LL - PL \tag{3.3}$$

3.2.5 Compaction characteristics: Compaction of clay specimens was conducted in accordance with the guidelines specified in BS 1377 (1990) to compute the required parameters. The reduced British Standard light (RBSL) compactive effort was used. The RBSL compaction is the energy resulting from 2.5 kg rammer falling through a height of 30 cm onto three layers of soil, each receiving 25 blows.

3.2.6 Free Swell Index of soil

This test was done to determine the free swell index of the soil samples and it has helped in identifying the swelling potential of the soil samples. This was done in accordance with guidelines specified in (BS 1377:1990; IS 2720: 1977).

It was calculated using equation 3.4.

$$FSI = \frac{V_d - V_k}{V_k} \times 100$$

(3.4)

Where:

FSI = Free swell index

V_d = The volume of soil specimen read from the graduated cylinder containing distilled water

V_k = The volume of soil specimen read from the graduated cylinder containing Kerosene.

Sridharan and Prakash (2000) classification for expansive soil chart was used to obtain the swelling potential or the rate of expansion of the soil at different depth. The kerosene absorbent test method was used to examine the free swell index of samples.

3.2.7 Consolidated undrained triaxial test (CU)

The CU test was conducted in accordance with the procedure specified in BS, 1377: (1990). The treated specimens were prepared relative to OMC and compacted with British Standard light compactive energy. The CU test was done using all round pressure of 50, 100 and 150 kN/m^2 different on soil sample specimens each of which was consolidated in three layers cycles.

The equipment used for consolidated undrained triaxial test is shown on Plate I

Plate I: Consolidated undrained test of samples

3.3 Model Raft Foundation Analysis

The analysis was conducted on a raft foundation of 40 meters long, 20 metres wide and 1.5 meters deep. Six loads of 5000 kN was applied on the foundation in two symmetrical gridlines. While modelling the raft foundation using Plaxis 3D, the model was modified so that the basement consists of structural elements. This allows for the calculation of structural forces in the foundation. The loads of the upper floors were transferred to the floor slab by a column and by the basement walls.

Figure 3.1 shows the dimensions of the foundation and the position where the loads were applied.

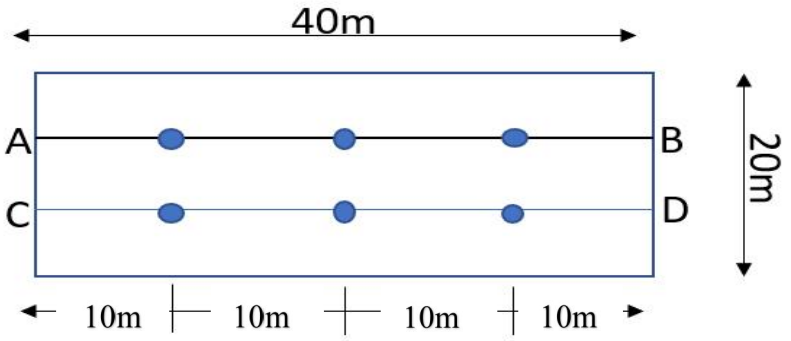

Figure 3.1: Loading points of modelled raft footing

CHAPTER FOUR

4.0 RESULTS AND DISCUSSION

4.1 Index Properties of The Soils

Tables for results of index properties of the soils are shown in Appendix A. The fraction passing through No 200 sieve for soil collected at depths 0m, 1m and 1.5m are 68.57%, 63.43% and 65.33% respectively. The soils are classified A-7-5 (CL), A-7-5 (CH) and A-7-6 (CH) at 0m, 1.0m and 1.5m depths respectively according to AASHTO and USC soil classification systems respectively (AASHTO, 1986; ASTM, 1992).

4.2 Natural Moisture Content

The results for natural moisture content are presented in Appendix B. The average moisture content at depth 0m, 1.0m and 1.5m are 17.55, 18.9 and 28.10 respectively.

It was observed that the natural moisture content increases with height due to exposure to atmosphere and also the closeness to water table.

4.3 Specific Gravity of Soil Sample

The results for specific soil samples are presented in Appendix C. The average specific gravity at depth 0m, 1.0m and 1.5m are 2.73, 2.57 and 2.77 respectively and this revealed that the soils are clayey soils.

4.4 Atterberg Limit Test

Atterberg limit results test results are presented in Appendix D. At depth 0m, the average liquid limit is 51% and the avaerage plastic limit is 30.77%. Therefore the PI at depth 0m is 20.23%.

At depth 1.0m, the average liquid limit is 55.80% and the avaerage plastic limit is 25.0%. Therefore the PI at depth 0m is 30.8%.

At depth 1.5m, the average liquid limit is 43.20% and the avaerage plastic limit is 29.63%. Therefore the PI at depth 0m is 13.57%.

It was observed soil at depth 1.0m has the highest PI which implies that the soil has the highest clay content.

4.5 Compaction Characteristics

The results for compaction characteristics are presented in appendix E. From the graph plotted, the MDD and OMC at depth 0m are 1.805g/cm^3 and 16% respectively. At depth 1.0m, the MDD and OMC are 1.785 g/cm^3 and 17.2% respectively and at depth 1.5m the MDD and OMC are 1.715 g/cm^3 and 20.95% respectively. It was observed that MDD decreases when the depth increases while OMC increases with depth.

4.6 Free Swell Index of Test Samples

The results of free swelling index of samples collected are shown in Appendix F

The average free swell index of the soil at 0-meter depth is 105.93%. Therefore, the soil, having a FSI of 105.93% (which falls between 95 – 120%) is highly expansive according to (Sridharan and Prakash, 2000).

The results of swelling index of samples collected from 1.0 metre depth are shown in Table 3. The average free swell index of the soil at 1.0m depth is 110.82%. Therefore, the soil at this depth, having a FSI of 110.82% (which falls between 95 – 120%) is highly expansive according to (Sridharan and Prakash, 2000).

The average free swell index for the soil at depth 1.5m is 118.17%. Therefore, the soil at this depth, having a FSI of 118.17% (which falls between 95 – 120%) is highly expansive according to (Sridharan and Prakash, 2000).

4.7 Consolidated undrained triaxial test (CU)

The following are the results obtained from the test and computation of the results of triaxial test of sample moulded using the MDD and OMC from British Standard Light compaction test according to BS 1377: 1990). The test was repeated for other samples collected from 0, 1.0 and 1.5m depth respectively. The results are shown in Tables 4.1 – 4.6 and Figures 4.1 – 4.4.

Table 4.1: Triaxial test results of samples at depth of 0m

Item	**Quantity**		
All round Pressure (kN/m^2)	50	100	150
Axial Deformation (mm)	400	600	525
Loading (N)	12	19	32

Table 4.2: Principal stresses of test samples at

σ_3(kN/m^2)	**σ_2(kN/m^2)**	**σ_1(kN/m^2)**
50	72	122
100	110	210
150	191	341

0m

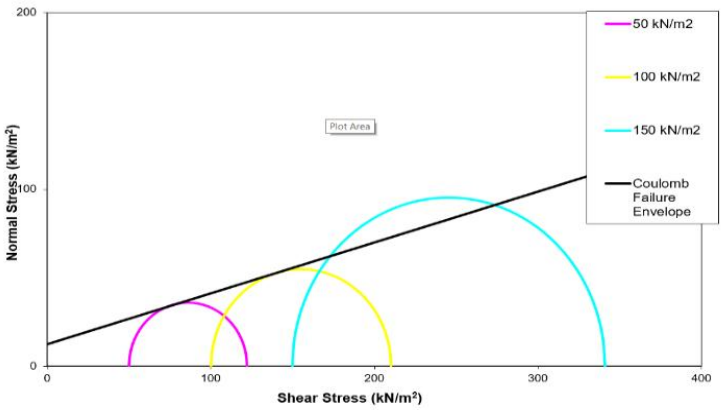

Figure 4.1: Mohr circle diagram of sample at 0 m

From the figure 41, it can be deduced that the cohesive strength of the soil 12.5 kN/m^2 and angle of internal friction is 23^0

Table 4.3: Triaxial test results of sample at 1.0m

Item	**Quantity**		
All round Pressure(kN/m^2)	50	100	150
Axial Deformation (mm)	400	525	425
Loading (N)	11.2	17	19.8

Table 4.4: Principal stresses for sample at 1.0m depth

σ_3(kN/m^2)	σ_2(kN/m^2)	σ_1(kN/m^2)
50	67	117
100	100	200
150	115	265

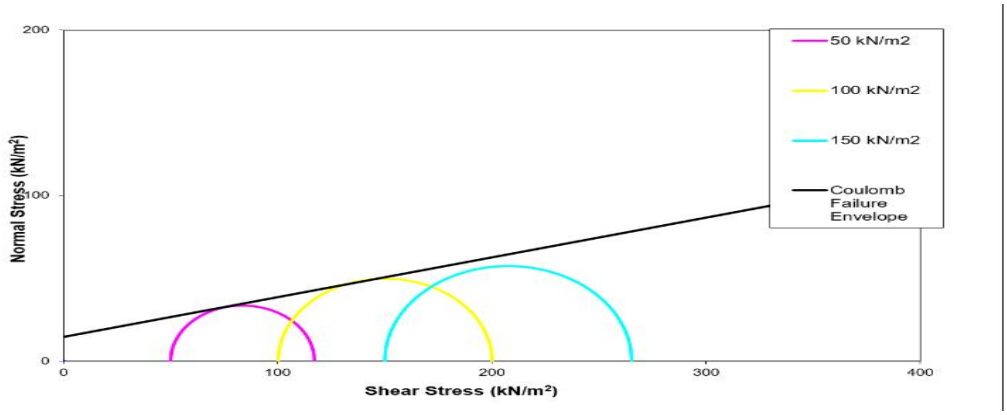

Figure 4.2: Mohr circle diagram of sample at 1.0m depth

Figure 4.2 revealed that the cohesive strength of the soil 14.7kN/m^2 and angle of internal friction is 23^0.

At the depth of 1.5m

Table 4.5: Triaxial test results of sample at 1.5m depth

Item	**Quantity**		
All round Pressure (kN/m^2)	50	100	150
Axial Deformation (mm)	475	525	625
Loading (N)	13.2	20.1	30

Table 4.6: Table from computation of the results

σ_3(kN/m^2)	σ_2(kN/m^2)	σ_1(kN/m^2)
50	78	128
100	118	218
150	173	323

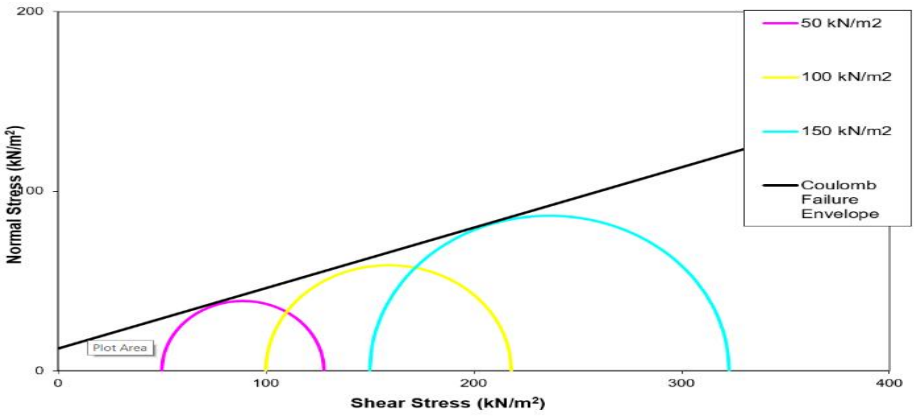

Figure 4.3: Mohr circle diagram of sample at 1.5m depth

Figure 4.3 revealed that the cohesive strength of the soil 12.7 kN/m^2 and angle of internal friction is 26^0.

Table 4.7 revealed the summary of the properties of the clay at different layers.

Table 4.7: Summary of properties of test clay

Properties (Average)	**Layer A (0m)**	**Layer B (1.0m)**	**Layer C (1.5m)**
Specific gravity (Gs)	2.73	2.57	2.77
Natural moisture content (%)	18.94	17.55	28.10
Atterberg Limits			
Liquid limit (%)	54.5	47.0	43.2
Plastic limit (%)	38.19	32.92	29.63
Shrinkage limit (%)	9.64	9.21	10.00
Plasticity index	16.31	14.08	13.57
% Passing BS No. 200 sieve	51.90	52.70	54.70
Classification			
USCS	CL	CH	CH
AASHTO	A-7-5	A-7-5	A-7-6

The summary of geotechnical properties of the critical test samples used for both Mohr-Coulomb model and Finite Element Analysis is shown in Table 4.7, while the discussion is presented thereafter.

4.8 Deformation of samples

4.8.1 Initial stage deformation

An increase deformation at the initial stage is shown in the interphase mesh in Plate II. The extreme deformation at this stage is 615.15 x10^{-6}m, which is lower than those of excavation and final stages. The load here is gradual and the soil around the foundation is stll within the elastic state, with little or minimum distortion of soil particles.

The deformation at this stage is show on Figure 4.4 and 4.5.

Table 4.8 revealed the deformation values across the distances.

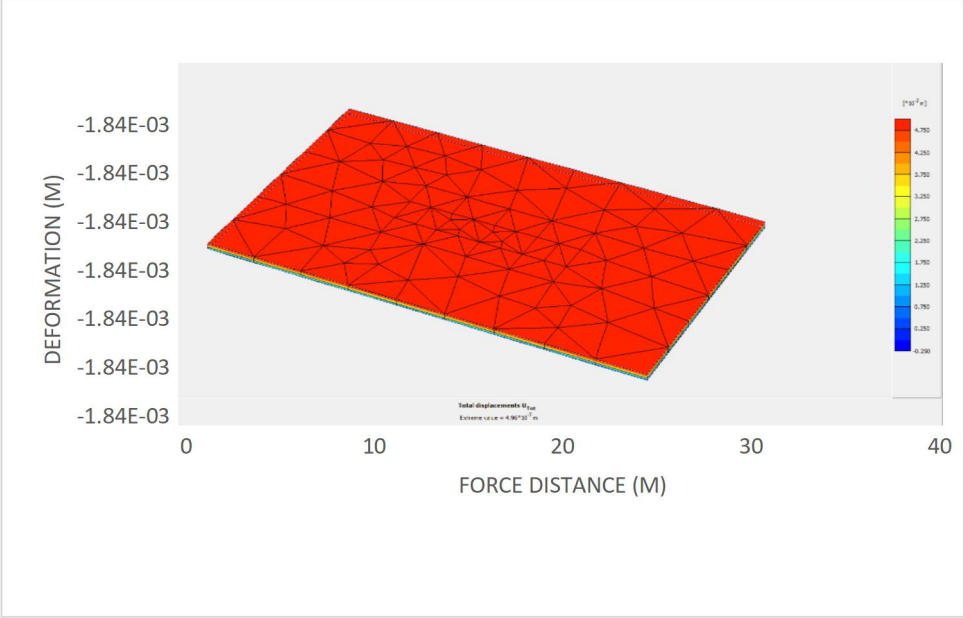

Figure 4.4: Initial stage deformation of the soil

Table 4.8: Initial stage deformation at loaded points

Distance	Deformation (m)	
	Line A-B	Line C-D
10	0.00061514	0.000615143
20	0.00061515	0.000615149
30	0.000615145	0.000615144

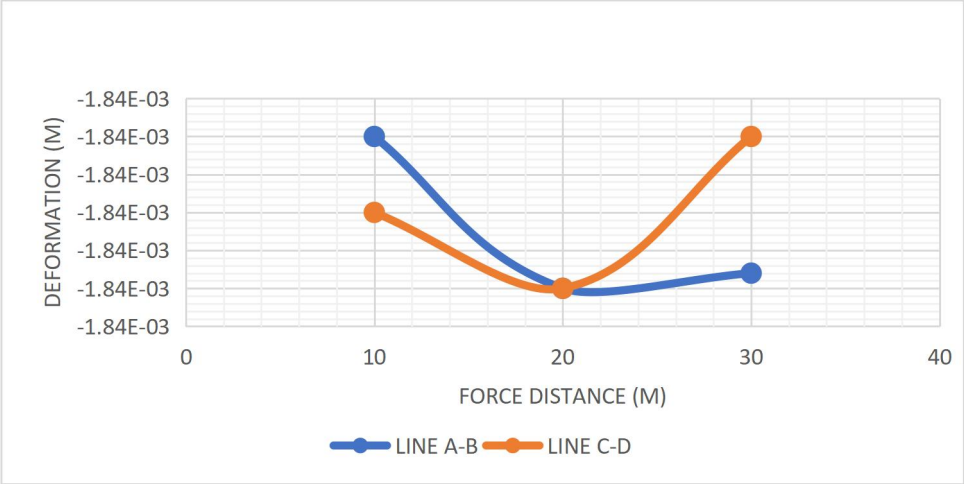

Figure 4.5: Initial stage deformation curves of loaded points

4.8.2 Excavation stage deformation

Due to the forces invloved in foundation excavation, the deformation at this stage increased due structural imbalance and particles phase distortion. Another factor, which contributed to the increase deformation is soil grain distabilization resulting from displacement, remoulding and other disturbnaces during soil during excavation. The highest increase in deformation caused be the threshold load at this stage is 4.55 $x10^{-3}$m.

The deformation at this stage is show on Figure 4.6 and 4.7.

Table 4.9 revealed the deformation values across the distances.

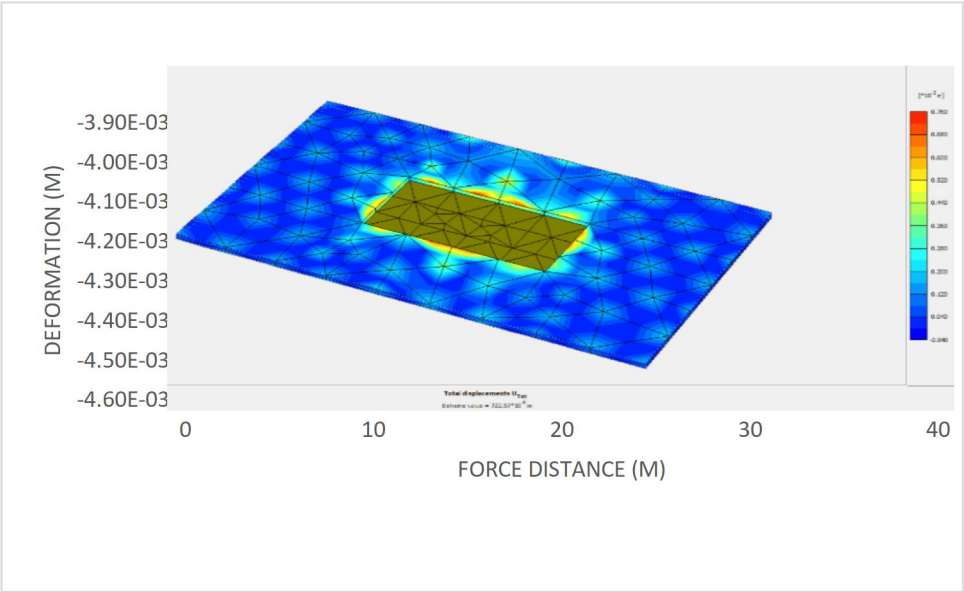

Figure 4.6: Excavation stage deformation of the soil

Table 4.9: Excavation stage deformation at loaded points

Distance(m)	Deformation (m)	
	Line A-B	Line C-D
10	0.004467	0.004550
20	0.004511	0.004012
30	0.004345	0.004365

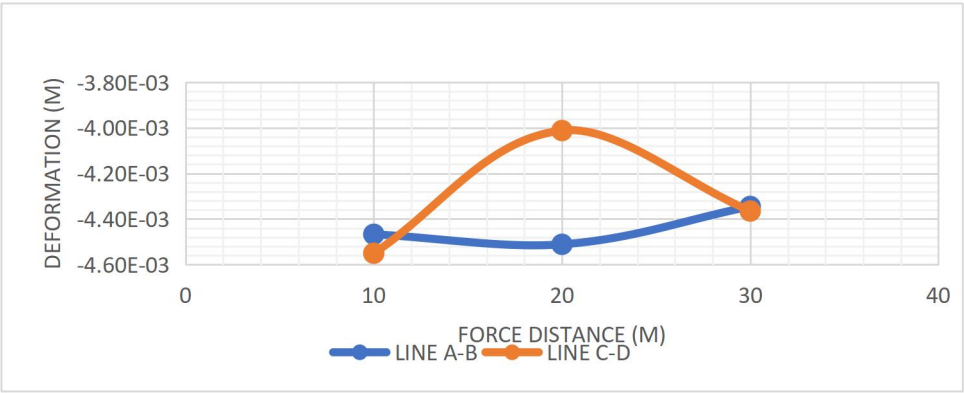

Figure 4.7: Excavation stage deformation curve of loaded points

4.8.3 Final Stage Deformation

A higher deformation of $4.55*10^{-3}$m occurred at the excavation stage. However, with the introduction of model raft, the total deformation at this stage reduced to 606.95

x10^{-6}m. The raft served as both stiffner and brace, thereby reducing the effect on surroundig soil.

The deformation at this stage is show on Figure 4.8 and 4.9.

Table 4.10 revealed the deformation values across the distances.

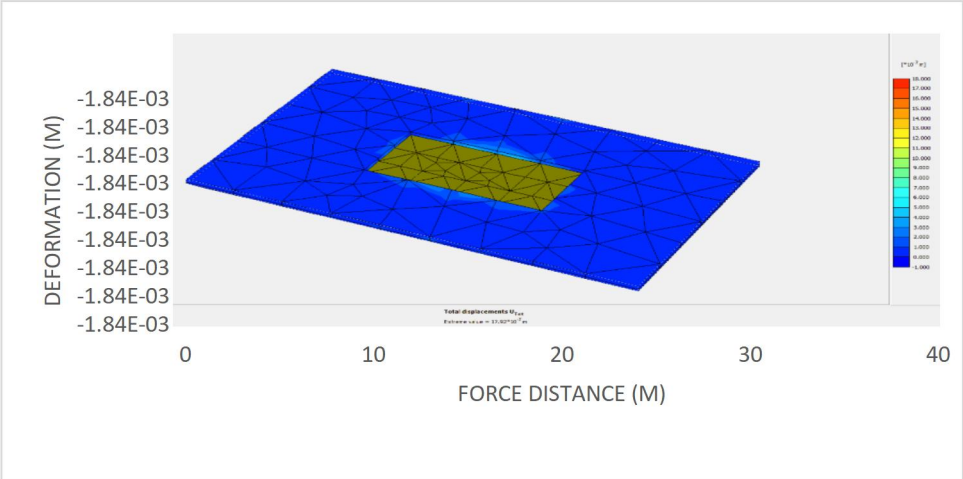

Figure 4.8: Final stage deformation of the soil

Table 4.10: Final stage deformation at loaded points

Distance(m)	Deformation(m)	
	Line A-B	Line C-D
10	0.00000606949	0.00000606949
20	0.00000606950	0.00000606950
30	0.00000606948	0.00000606948

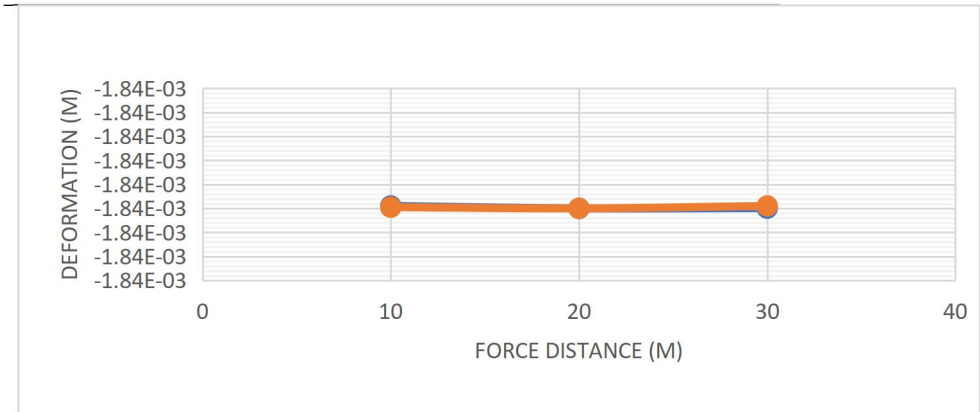

Figure 4.9: Final stage deformation curve of loaded points

CHAPTER FIVE

5.0 CONCLUSION AND RECOMMENDATIONS

5.1 Conclusion

From the results of Finite Element Analysis of raft foundation load-bearing response in expansive clay, the following conclusions were drawn;

The free swell index (*FSI*) of test clay samples collected from 0 – 1.5 meters depth raged from 105.95 to 118.18%, which classified it under highly expansive clay.

Higher deformation of the soil, which was due to disturbance and distortion was recorded at the excavation stage than the one recorded at initial stage with values of 4.55 $x10^{-3}$m and 615.15 $x10^{-6}$m respectively.

With the introduction of model raft, the total deformation at excavation stage reduced to 602.01 $x10^{-6}$m, with the raft serving as both stiffner and brace.

5.2 Recommendations

1. Finite element analysis is recommended for analysis of foundation failure especially in expansive clay.
2. Further research may be carried out on the sensitivity to cyclic loading on foundation in expansive soil.

5.3. Contribution to Knowledge

This thesis showed that Plaxis 3D can be used to analysis raft foundation in soils with low bearing capacity. The work established an 86.77% reduction in deformation with introduction of modelled raft which served as stiffener and brace.

REFERENCES

Alnuaim, A.M, El Naggar, H. & El Naggar, M.H. (2013). Performance of piled-raft system under axial load. *Proceedings of the 18th International Conference on soil mechanics and Geotechnical Engineering*, Paris. 2663-2666

Ameta, N. K., Purohit D.G. M., & Wayal, A. S. (2007). Characteristics, Problems and Remedies of Expansive Soils of Rajasthan, *EJGE* India.

Argyris, J. H. (1965). Continua & Discontinua. *Proceedings, Conference on Matrix Methods in Structural Mechanics*, Wright-Patterson A.F.B., Ohio, pp. 11-189.

Argyris, J. H. & Kelsey, S. (1955). Energy Theorems and Structural Analysis. *Aircraft Engineering,* Vols. 26 and 27

Al-Ansari, M, Sadeq, H. A., & SaleemTaha, M. (2009), "Structural Design of Raft Foundation", Qatar University college of engineering.

Al-Damluji, O. S. & Al-Baghadadi, N. H. (2012). Analysis of piled-raft foundation by the finite element method. *Kufa Journal of Engineering, Iraq.* 3,115-132

Al-Rawas, A. A., Hago, A. W., & Al-Sarmi, H. (2005). Effect of lime, cement and Sarooj (artificial pozzolan) on the swelling potential of an expansive soil from Oman, *Built Environment.,* 40(5), 681–687.

Berezantzev, V. G., Khristoforov, V. and Golubkov, V., (1961). Load bearing capacity anddeformation of piled foundations. *Proc. 5th Int. Conf. Soil Mech. Fdn Engng*, Paris. 2, 11-15.

Burland, J. B., (1973). Shaft friction of piles in clay: a simple fundamental approach. *Ground Engng*, 6(3), 30 - 42.

Burland, J. B., Broms, B. B. and De Mello, V. B. (1978). Behaviour of foundations and structures. *Proc. 9th ICSMFE*. Tokyo: 2, 496-546.

Chen, F.H. (1988). Foundations on Expansive Soils. *Elsevier Scientific Publishing Company*, Amsterdam.

Chow, Y. K. (1989). Axially Loaded Piles and Pile Groups embedded in a cross-anisotropic Soil. *Géotechnique*, 39(2), 203-211.

Clough, R. W. (1960). The Finite Element Method in Plane Stress Analysis. *Proceedings, Second ASCE Conference on Electronic Computation*, Pittsburgh, PA, 345-378.

Conte, E., Donato, A. & Troncone, A**.** (2013). Progressive failure analysis of shallow foundations on soils with strain-softening behaviour**.** *Computers and Geotechnics*. 54,117–124

Courant, R. (1943). Variational Methods for the Solution of Problems of Equilibrium and Vibrations. *Bulletin of the American Mathematical Society*. 49, 1-23.

Dang, L. C, Fatahi, B. & Khabbaz, H. (2016). Behaviour of Expansive Soils Stabilized with Hydrated Lime and Bagasse Fibres. *Procedia Eng*. 143, 658–665.

Das, A. & Roy, S., (2014). Effect of expansive soil on foundation and its remedies. *International Journal of Innovative Research in Science, Engineering and Technology*. 3, 92-95.

De-Weck, O. & Kim, I. Y. (2004). Finite Element Method. *Engineering Design and Rapid Prototyping.* Massachusetts Institute of Technology. 1-26

Fellenius, B. H. (2004). UNIPILE Design on Piled Foundations with Emphasis on Settlement Analysis. *Journal of the Soil Mechanics and Foundations Division*, ASCE, 125(GSP), 1-23.

Fleming, W. G. K., Weltman, A. J., Randolph, M. F. & Elson, W. K. (1992). Piling Engineering. 2nd Ed., *Surrey University Press,* Surrey, United Kingdom

Garba, M. A. (2014). Optimum design of reinforced concrete raft foundations using finite element analysis. *a thesis submitted to the school of postgraduate studies, Ahmadu Bello University, Zaria*

Grim, R.E. (1950). Modern Concepts of clay Materials. *Journal of Geology*. L:225-275

Grim, R.E. (1962). Applied Clay Mineralogy. Publisher: *McGraw Hill*, the University of California, USA

Guggenheim, E., Stephen, A. and Martin (1995). Definition of clay and clay mineral. *Journal Report of the AIPEA nomenclature and CMS nomenclature committees.* Pg 255-256

Guney, Y., Sari, D., Cetin, M. and Tuncan, M, (2007). Impact of cyclic wetting-drying on swelling behaviour of lime stabilized soil. *Handbook on Environments Chem*icals Vol. 5 Water Pollution. 42 (2), 681–688.

Gupta, S. C. (2007). Raft Foundation (Design and Analysis with a Practical Approach). *New Age International Publishers.* USA

Halkude, S. A., Kalyanshetti, M. G., Barelikar S.M (2014). Seismic response of R.C. frames with raft footing considering soil structure interaction. *International Journal of Current Engineering and Technology*. 4(3), 222-236

Hewitt, P. B. & Gue, S. S. (1994). Piled Raft Foundation in a weathered sedimentary formation. *Proceeding Geotropica*, Malaysia, 1-1.

Hutton, D. V. (2004). Fundamentals of finite element analysis. 1st ed. *Mc Graw Hill.* New York, USA.

Jawad, T. A. (1998). Optimization of Raft Foundation Design. *MSc thesis*, University of Technology, USA.

Johnson L. D. (1969). Review of literature on expansive clay soils. *Miscellaneous paper S-69-24.* Army-Mrc, Vickbburq, Mississippi.

Johnson, K., Christensen, M., Sivakugan, N. & Karunasena, W. (2015). Simulating the Response of Shallow Foundations using Finite Element Modelling School of Engineering, James Cook University, Townsville, Queensland, 4811, Australia.

Khemissa, M. & Mahamedi, A. (2014). Cement and lime mixture stabilization of an expansive overconsolidated clay. *Applied Clay Science*, 95, 104–110.

Kitiyodom, P. & Matsumoto, T. (2003). A Simplified Analysis Method for Piled Raft Foundations in Non-homogeneous Soils. *Int. J. Numer. Anal. Meth. Geomechanics*., 27:85-109.

Kraskiewicz, C., Michalczyk R., Brezinski K. & Pludowska M. (2015). Finite Element modelling and design procedures for verifications of trackbed structure. *Procedia Engineering 111*, 462 – 469

Lates, E. M., Elmonshid, B. E. F. & Abbo, S. H. (1983). Review of Problems Generated by Expansive Sols in Sudan. *Proc. Of Seminar on Expansive Clay Soils Problems in Sudan*, Wad Medani, Hydraulic Research Station, HRS

Lee, W. J., Lee, I. M., Yoon, S.J., Choi, Y. J. & Kwon, J. H. (1996). Bearing Capacity Evaluation of the Soil-Cement Injected Pile Using CAPWAP. *Proc. of the 5th Int. Conf. on the Application of Stressway Theory to Piles*. University of Florida, Orlando Florida USA.

Liang, F. Y., Chen, L. Z. & Shi, X. G. (2003). Numerical Analysis of Composite Piled Raft with Cushion Subjected to Vertical Load. *Computers and Geotechnics*. 30, 443-453.

Mardia, M. (2014). Finite Element Analysis of Elastic Settlement of Shallow Foundation. *MSc Thesis,* Bangladesh University of Engineering and Technology, Bangladesh.

Mestat, P. (1990). Méthodologie de détermination des paramètres des lois de comportement des sols à partir d'essais triaxiaux conventionnels, 1(16) 176-195.

Mestat, P. (1993). Lois de comportement des géomatériaux et modélisation par la méthode des éléments finis, Etudes et recherches des laboratoires des ponts et chaussées, GT 52, 193 p.

Meyerhof, G. G. (1976). Bearing Capacity and Settlement of Pile Foundation. *Journal of the Soil Mechanics and Foundations Division,* ASCE, 102(GT3), 197-228.

Mohammed, S. A. (2017). Structural Behaviour of tall building Raft foundation in Earthquake Zones: *Open Journal on Earthquake Research*. 180-190.

Mughieda, O. & Hazirbaba, K. (2015). Expansive Clay Soil-Structure Interaction: A Case Study, Recent Advances in Mechanics, Mechatronics and Civil,

Chemical and Industrial Engineering, *Proceedings of the International Conference on Civil Engineering*. 195-200

Nova, R. (1982). A model of soil behaviour in plastic and hysteretic ranges. *Int. Workshop on Constitutive Behaviour of Soils,* Grenoble. 289-306.

Oh, E.Y., Huang, M., Surarak C., Adamec R. & Balasurbamaniam A. S. (2008**).** Finite Element Modelling for Piled Raft Foundation in Sand. *Eleventh East Asia-Pacific Conference on Structural Engineering & Construction (EASEC-11) "Building a Sustainable Environment"* Taipei, TAIWAN EASEC-11

Patil, S.S., Kalyanshetti, M. G, & Dyawarkonda, S. S. (2016). Parametric study of R.C frame with raft foundation considering soil structure interaction using spring. *International Journal of science and Engineering Development Research.* 1(4)

Poulos, H. G. (1989). Pile Behaviour – Theory and Application. *Géotechnique*, 39(3), 365-415.

Poulos, H. G. (1991). Analysis of Piled Strip Foundations. *Computation Methods and Advances in Geomechs*., Rotterdam, 1, 183-191

Popa, H. & Batali, L. (2010). Using Finite Element Method in geotechnical design. Comparison between soil constitutive laws and case study. *Proceedings of the 3rd WSEAS Int. Conference on finite differences*. 228-233

Prakoso, W. A. & Kulhawy F. H. (2001). Contribution to Piled Raft Foundation Design. *Journal of Geotechnical and Geoenvironmental Engineering, ASCE*, 127(1), 17-24.

Pusadkar, S. S. & Bhatkar, T. (2013). Behaviour of Raft Foundation with Vertical Skirt Using Plaxis 2d. *International Journal of Engineering Research and Development*. 7(6), 20-24

Reese, L. C. & O'Neill, M. W. (1989). New Design Method for Drilled Shaft from Common Soil and Rock Test. *Proceedings of Congress Foundation Engineering: Current Principles and Practices,* ASCE, 2, 1026-1039.

Reul, O. & Randolph, M. F. (2003). Piled Rafts in Overconsolidated Clay: Comparison of in situ Measurements and Numerical Analysis. Géotechnique, 53(3), 301-315.

Rogers, D., Olshansky, R., & Robert, B. (1985). Damage to foundations from expansive soils. *PhD Dissertation.* Missouri University of Science and Technology, Missouri.

Russo, G. (1998). Numerical Analysis of Piled Rafts. *International Journal for Numerical Analytical Methods and Geometrics.* 22, 477-493.

SaadEldin, M. & El-Helloty, A. (2014). Effect of Opening on Behaviour of Raft Foundations Resting on Different Types of Sand Soil. *International Journal of Computer Applications*. 94(7).

Salah, R. A., Aqeel T. F., & Omar K. A. (2015). Using Finite Element to Modify Winkler Model for Raft Foundation Supported on Dry Granular Soils: *International Journal of Science and Research (IJSR):* 2319-7064

Samtani, N. C. & Nowatzki, E. A. (2006). Soils and Foundations. *Federal Highway Administration Publication,* "Reference Manual – I,.

Sarkar, G. & Islam, M. (2012). "Study on the Geotechnical Properties of Cement based Composite Fine-grained Soil," *International Journal for Advance Structural and Geotechnical Eng*ineers,1(2,).

Semple, R. M. & Rigden, W. J. (1984). Shaft capacity of driven piles in clay, *Proceedings of the symposium on analysis and design of pile foundations,* San Francisco, 59–79.

Shihada, E & Hamad, S (2008). Modifications of Conventional Rigid and Flexible Methods for Mat Foundation Design. *Islamic University of Gaza*, Civil Engineering Department.

Small, J. C. & Zhang, H. H. (2000). Piled Raft Foundation Subjected to General Loading. *Developments in Theoretical Geomechanics*. Balkema, Rotterdam, 57-72.

Srivastava, A., Goyal, C. R. & Jain A. (2012). Review of causes of foundation failures and their possible preventive and remedial measures. *International Engineering conference,* Thailand, pp 1-6.

Subramanian, N. (2009). Rare foundation failure of a building in Shanghai: *China consulting engineer*, Gaithersburg, Maryland, USA**,** 100-105

Synge, J. L. (1957). The Hypercircle in Mathematical Physics*, Cambridge University Press,* London.

Terzaghi, K. & Peck, R.B. (1948). Soil mechanics in engineering practice. *John Wiley and Sons Inc*., New York, USA.

Turner, M. J., Clough, R. W., Martin, H. C., & Topp, I. J. (1956). Stiffness and Deflection Analysis of Complex Structures. *Journal of the Aeronautical Sciences*, 23:805-823.

Wang, J. W. (2016). Expansive soils and practice in foundation engineering. *Louisiana Transportation Conference,* Baton Rouge. 1-79.

Wentworth, C. K. (1922). A Scale of Grade and Class Terms for Clastic Sediments. *The Journal of Geology,* 30(5),377-392

Vermeer, P. (1982). A five constant model unifying well established concepts. *International workshop on Constitutive Behaviour of Soils,* Grenoble, 175-197

Vesic, A. S. (1972). Expansion of Cavities in Infinite Soil Mass. *Journal for Soil Mechanics and Foundations Div.* ASCE. 98, 265-290.

Yenes M., Nespereira J., Blanco J. A., Suarez M., Monterrubio S. & Iglesias C. (2012). Shallow foundations on expansive soils: a case study of the El Viso Geotechnical Unit, Salamanca, Spain. *Bulletin of Engineering Geology and Environment,* 71, 51–59.

Zienkiewicz, O. C., & Cheung, Y. K. (1967). The Finite Element Method in Structural and Continuum Mechanics*, McGraw-Hill*, New York, *USA.*

APPENDICES

APPENDIX A: Sieve Analysis Results of Samples

Table A1: Sieve analysis results for clay soil at depth 0m

Diameter (mm)	Soil Retained (g)	Soil Retained (%)	Soil Passing (%)
5.00	11.0	11.7	88.3
3.35	8.5	9.0	79.3
2.36	5.7	6.0	73.3
2.00	1.4	1.5	71.8
1.18	9.5	10.1	61.7
0.85	7.6	8.1	53.7
0.60	10.4	11.0	42.6
0.43	8.4	8.9	33.7
0.300	6.7	7.1	26.6
0.150	17.1	18.1	8.5
0.075	8.0	8.5	0.0
Pan	0.0	0.0	0.0
	94.3	100.0	

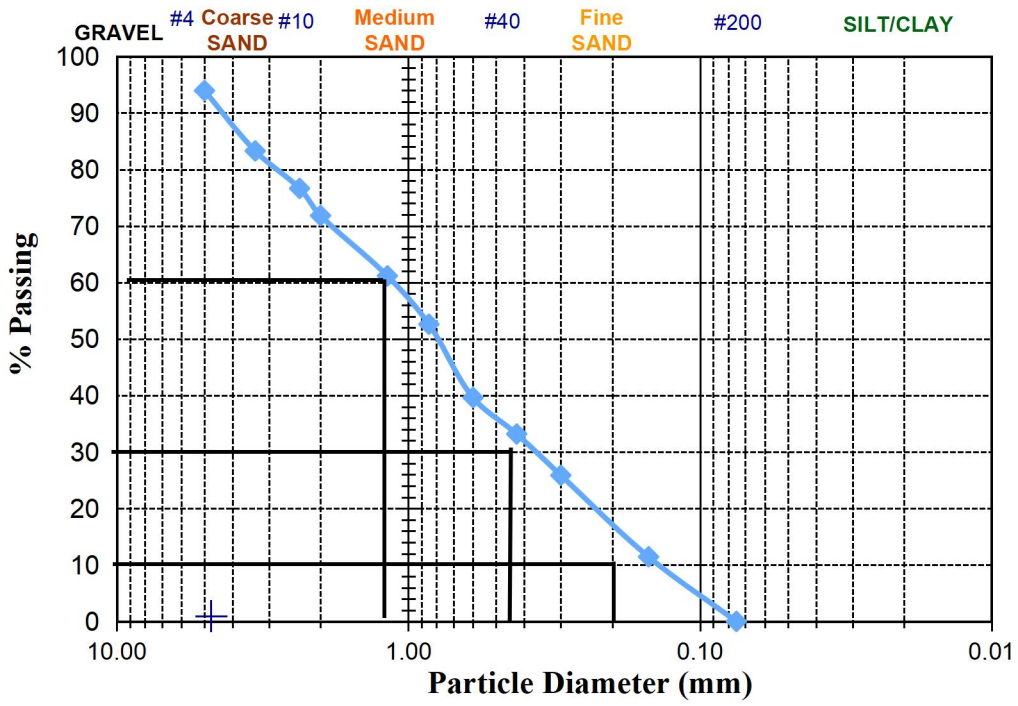

Table A2: Sieve analysis results for clay soil at depth 1.0m

Diameter (mm)	Soil Retained (g)	Soil Retained (%)	Soil Passing (%)
5.00	9.0	8.2	91.8
3.35	6.0	5.5	86.3
2.36	6.9	6.3	80.0
2.00	3.4	3.1	76.9
1.18	9.5	8.7	68.3
0.85	8.9	8.1	60.2
0.60	11.0	10.0	50.1
0.43	8.4	7.7	42.5
0.300	7.6	6.9	35.6
0.150	23.6	21.5	14.0
0.075	15.4	14.0	0.0
Pan	0.0	0.0	0.0
	109.7	**100.0**	

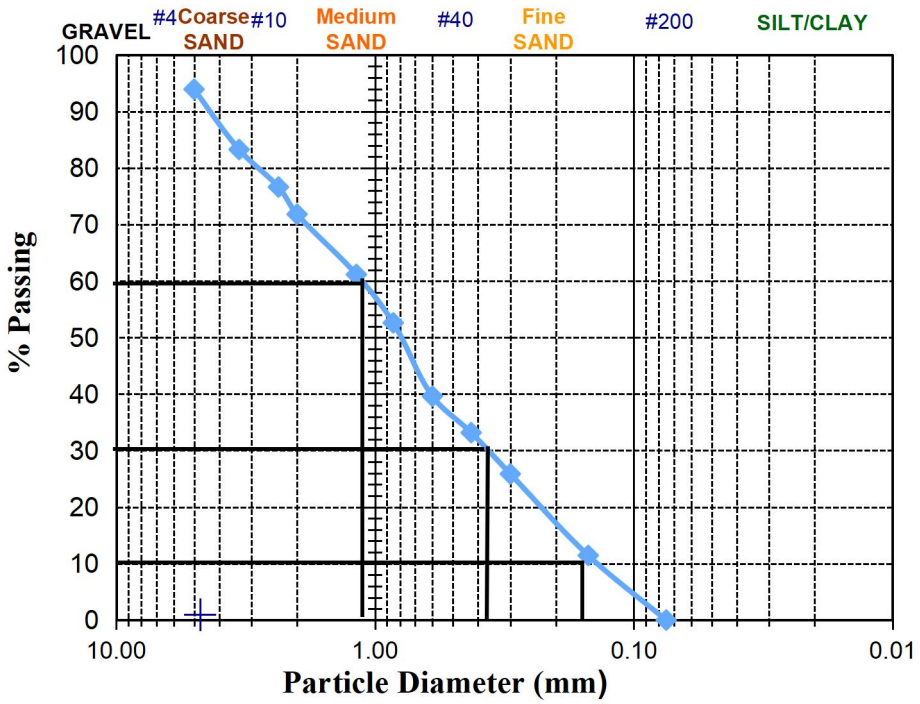

Table A3: Sieve analysis results for clay soil at depth 1.5m

Diameter (mm)	Soil Retained (g)	Soil Retained (%)	Soil Passing (%)
5.00	6.3	6.1	93.9
3.35	11.1	10.7	83.3
2.36	6.9	6.6	76.6
2.00	5.0	4.8	71.8
1.18	11.1	10.7	61.2
0.85	8.9	8.6	52.6
0.60	13.5	13.0	39.6
0.43	6.7	6.4	33.2
0.300	7.6	7.3	25.9
0.150	15.0	14.4	11.4
0.075	11.9	11.4	0.0
Pan	0.0	0.0	0.0
	104	100.0	

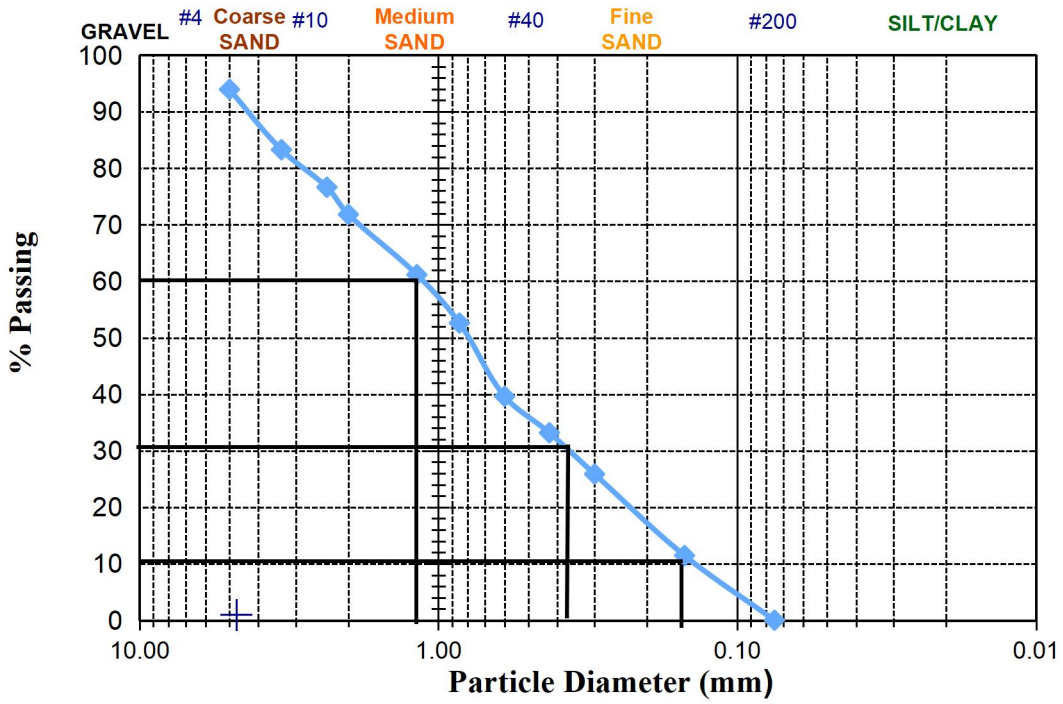

APPENDIX B: Natural Moisture Content of Samples

Table B1: Natural moisture content for clay soil at depth 0m

Can Weight (g)	38.40	38.70	35.30
Can Weight + wet soil (g)	150.00	149.70	150.30
Can Weight + Dry soil (g)	133.60	132.80	133.20
Weight Moisture (g)	16.40	16.90	17.10
Weight of Dry soil (g)	95.20	94.10	97.90
Moisture content (%)	17.23	17.96	17.47
		17.55	
Average Moisture Content			

Table B2: Natural moisture content for clay soil at depth 1.0m

Can Weight (g)	**38.40**	**38.00**	**24.80**
Can Weight + wet soil (g)	127.40	94.60	94.60
Can Weight + Dry soil (g)	113.90	85.60	95.70
Weight Moisture (g)	13.50	9.00	14.20
Weight of Dry soil (g)	75.50	47.60	70.90
Moisture content (%)	17.88	18.91	20.03
Average Moisture Content =		18.94	

Table B3: Natural moisture content for clay soil at depth 1.5m

Can Weight (g)	23.50	24.50	25.00
Can Weight + wet soil (g)	117.00	127.20	135.60
Can Weight + Dry soil (g)	96.50	104.70	111.30
Weight Moisture (g)	20.50	22.50	24.30
Weight of Dry soil (g)	73.00	80.20	86.30
Moisture content (%)	28.08	28.05	28.16
Average Moisture Content =		28.10	

APPENDIX C: Specific Gravity of Soil Sample

Table C1: Specific gravity of clay soil at depth 0m

No. of Trial	1	2
Weight of empty bottle	116.50	69.10
Weight of empty bottle + sample	181.20	100.90
Weight of empty bottle + sample + water	400.40	188.00
Weight of empty bottle + water	358.70	168.20
Specific Gravity	2.81	2.65
Average Specific Gravity	2.73	

Table C2: Specific gravity of clay soil at depth 1.0m

No. of Trial	1	2
Weight of empty bottle	116.50	69.10
Weight of empty bottle + sample	184.80	107.80
Weight of empty bottle + sample + water	400.30	191.90
Weight of empty bottle + water	358.70	168.20
Specific Gravity	2.56	2.58
Average Specific Gravity	2.57	

Table C3: Specific gravity of clay soil at depth 1.5m

No. of Trial	1	2
Weight of empty bottle	116.60	69.10
Weight of empty bottle + sample	178.70	102.70
Weight of empty bottle + sample + water	399.10	189.30
Weight of empty bottle + water	358.70	168.20
Specific Gravity	2.86	2.69
Average Specific Gravity	2.77	

APPENDIX D: Atterberg Limit of Soil Samples

Table D1: Atterberg limit of clay soil at depth 0m

	LIQUID LIMIT DETERMINATION						
	LIQUID LIMIT					**PLASTIC LIMIT**	
Trial Number	1	2	3	4	5	1	2
Penetration (mm)	7.10	11.70	17.30	20.20	26.00		
Wt. Of wet soil + can	41.10	42.00	43.20	43.70	46.10	39.70	39.90
Wt. Of dry soil + can	40.70	40.90	41.70	42.00	43.10	39.30	39.50
Wt. Of can	38.80	38.40	38.60	38.70	37.80	38.00	38.20
Wt. Of dry soil	1.90	2.50	3.10	3.30	5.30	1.30	1.30
Wt. Of water	0.40	1.10	1.50	1.70	3.00	0.40	0.40
Water content %	21.05	44.00	48.39	51.52	56.60	30.77	30.77
Liquid limit %	51.00		Average Plastic Limit			30.77	

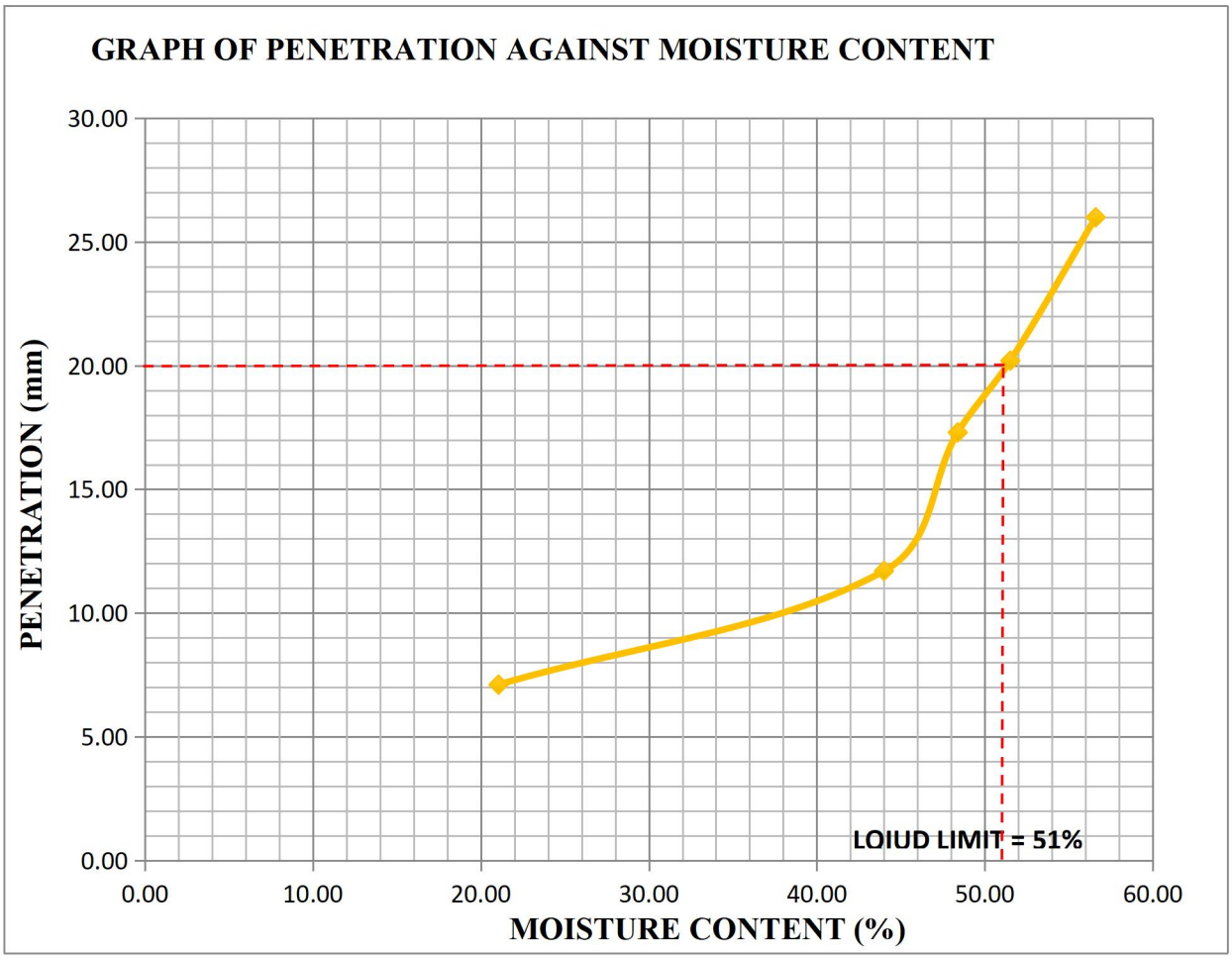

Table D2: Atterberg limit of clay soil at depth 1.0m

	LIQUID LIMIT DETERMINATION						
	LIQUID LIMIT					**PLASTIC LIMIT**	
Trial Number	1	2	3	4	5	1	2
Penetration (mm)	9.10	12.00	14.80	19.50	24.00		
Wt. Of wet soil + can	22.00	27.70	26.60	45.80	33.30	26.00	26.10
Wt. Of dry soil + can	21.40	26.10	25.30	43.10	30.30	25.80	25.80
Wt. Of can	18.60	22.00	22.50	38.20	25.30	24.80	24.80
Wt. Of dry soil	2.80	4.10	2.80	4.90	5.00	1.00	1.00
Wt. Of water	0.60	1.60	1.30	2.70	3.00	0.20	0.30
Water content %	21.43	39.02	46.43	55.10	60.00	20.00	30.00
Liquid limit %	55.80		Average Plastic Limit			25.00	

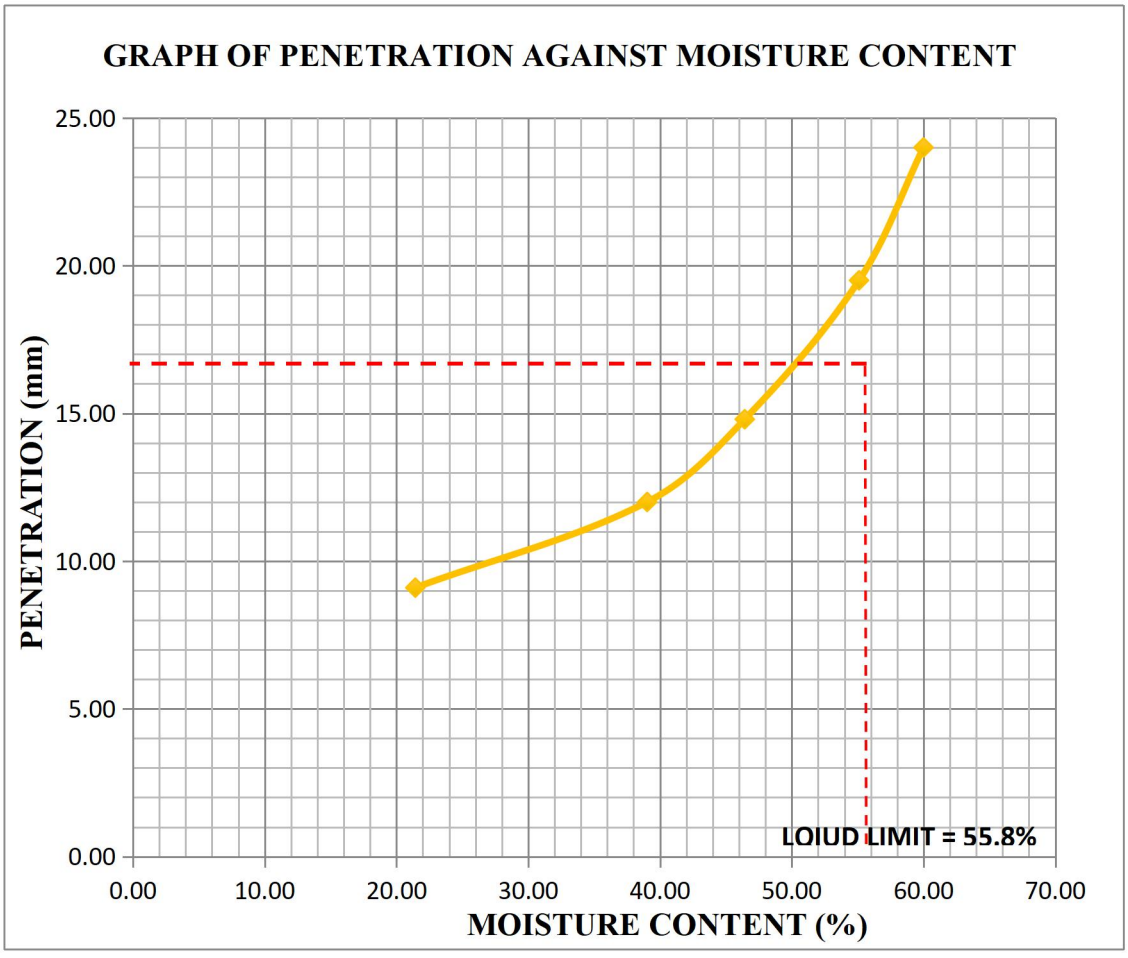

Table D3: Atterberg limit of clay soil at depth 1.5m

	LIQUID LIMIT DETERMINATION						
	LIQUID LIMIT					**PLASTIC LIMIT**	
Trial Number	1	2	3	4	5	1	2
Penetration (mm)	10.80	12.70	18.80	26.40	28.00		
Wt. Of wet soil + can	43.40	44.80	50.80	56.00	54.10	45.10	33.40
Wt. Of dry soil + can	42.60	43.50	47.30	50.40	49.00	43.40	31.50
Wt.Of can	38.80	38.60	39.00	38.20	38.30	37.90	24.80
Wt. Of dry soil	3.80	4.90	8.30	12.20	10.70	5.50	6.70
Wt.Of water	0.80	1.30	3.50	5.60	5.10	1.70	1.90
Water content %	21.05	26.53	42.17	45.90	47.66	30.91	28.36
Liquid limit %	43.20		Average Plastic Limit			29.63	

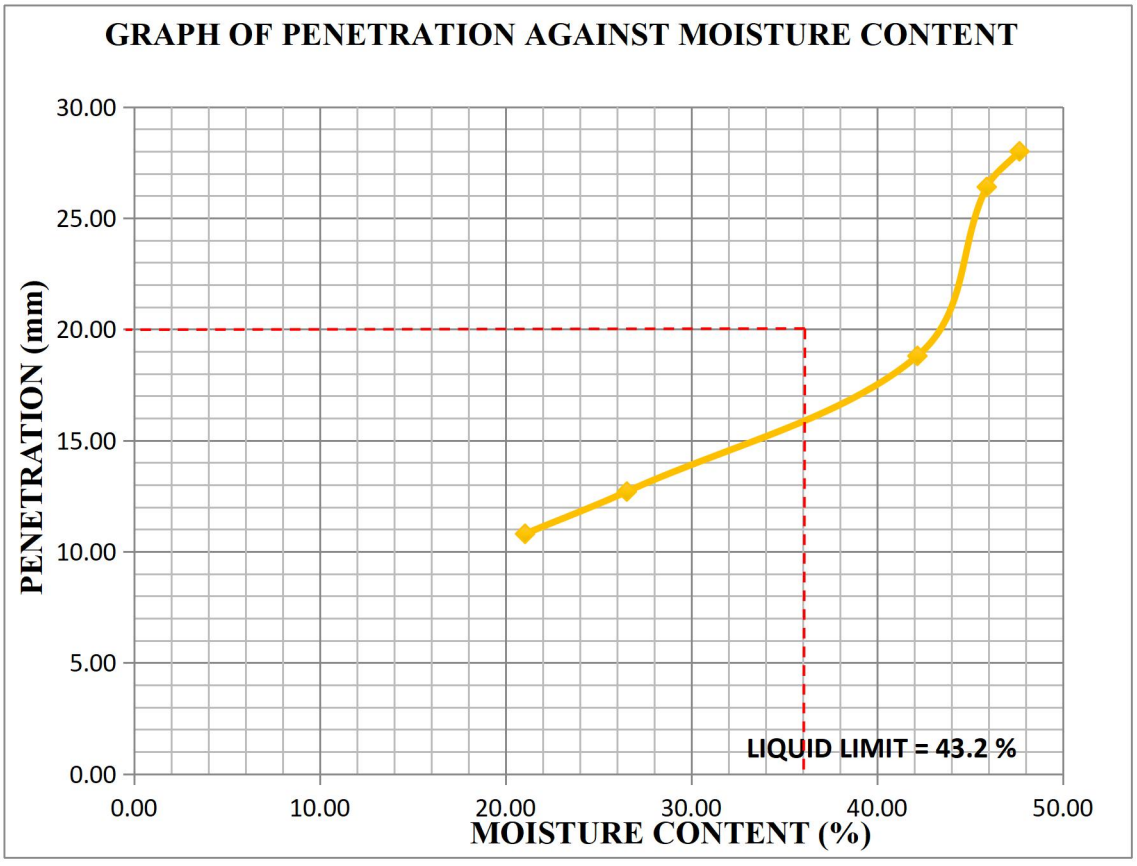

Appendix E: Compaction Characteristics of Soil Samples

Table E1: Compaction characteristics of clay soil at depth 0m

TEST DATA										
Mold No.	OB		ABX		YA		17			
Wt. Wet Sample + Mold	5525		5616		5700		5670		**5635**	
Wt. of Mold	3703		3703		3703		3703		**3703**	
Wt. of wet Sample	1822		1913		1997		1967		**1932**	
Volume of sample	944		944		944		944		**944**	
Wet Density	1.93		2.03		2.12		2.08		2.05	
Cont. No.	1	2	3	4	5	6	7	8	**9**	**10**
Wt. Wet Sample + Cont.	44.60	51.90	63.80	63.00	50.20	47.30	54.80	62.40	**53.30**	**45.90**
Wt. Dry Sample + Cont.	42.60	49.20	60.60	59.70	46.30	43.90	49.50	55.70	**47.70**	**41.80**
Wt. Water	2.00	2.70	3.20	3.30	3.90	3.40	5.30	6.70	5.60	4.10
Wt. Cont.	25.10	24.40	38.40	38.30	24.10	24.40	25.40	24.50	**24.60**	**24.60**
Wt, Dry Sample	17.5	24.8	22.2	21.4	22.2	19.5	24.1	31.2	23.1	17.2
Moisture Content %	11.4	10.9	14.4	15.4	17.6	17.4	22.0	21.5	24.2	23.8
Average moisture content %	11.16		14.92		17.50		21.73		24.04	
Dry Density	1.74		1.76		1.80		1.71		1.65	

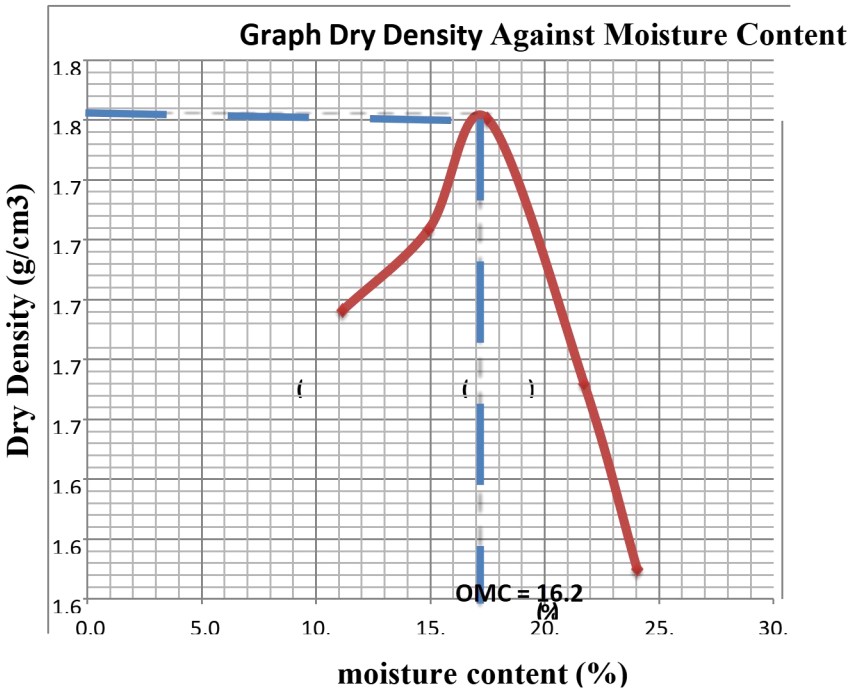
Graph Dry Density Against Moisture Content
Dry Density (g/cm3)
1.8
1.8
1.7
1.7
1.7
1.7
1.7
1.6
1.6
1.6
OMC = 16.2
0.0
5.0
10.
15.
20.
25.
30.
moisture content (%)

Table E2: Compaction characteristics of clay soil at depth 1.0m

TEST DATA										
Mold No.	OB		ABX		YA		17			
Wt. Wet Sample + Mold	5477		5555		5661		5655		**5575**	
Wt. of Mold	3703		3703		3703		3703		**3703**	
Wt. of wet Sample	1774		1852		1958		1952		**1872**	
Volume of sample	944		944		944		944		**944**	
Wet Density	1.88		1.96		2.07		2.07		1.98	
Cont.No.	1	2	3	4	5	6	7	8	**9**	**10**
Wt. Wet Sample + Cont	65.20	59.20	67.20	61.80	63.50	64.60	64.50	63.20	**63.30**	**64.80**
Wt. Dry Sample + Cont.	61.80	56.60	63.40	58.30	59.10	60.20	59.60	58.20	**57.80**	**59.20**
Wt. Water	3.40	2.60	3.80	3.50	4.40	4.40	4.90	5.00	5.50	5.60
Wt. Cont.	38.00	38.80	38.90	38.20	38.80	38.90	38.20	38.80	**38.30**	**39.90**
Wt, Dry Sample	23.8	17.8	24.5	20.1	20.3	21.3	21.4	19.4	19.5	19.3
Moisture Content %	14.3	14.6	15.5	17.4	21.7	20.7	22.9	25.8	28.2	29.0
Average moisture content %	14.45		16.46		21.17		24.34		28.61	
Dry Density	1.64		1.68		1.71		1.66		1.54	

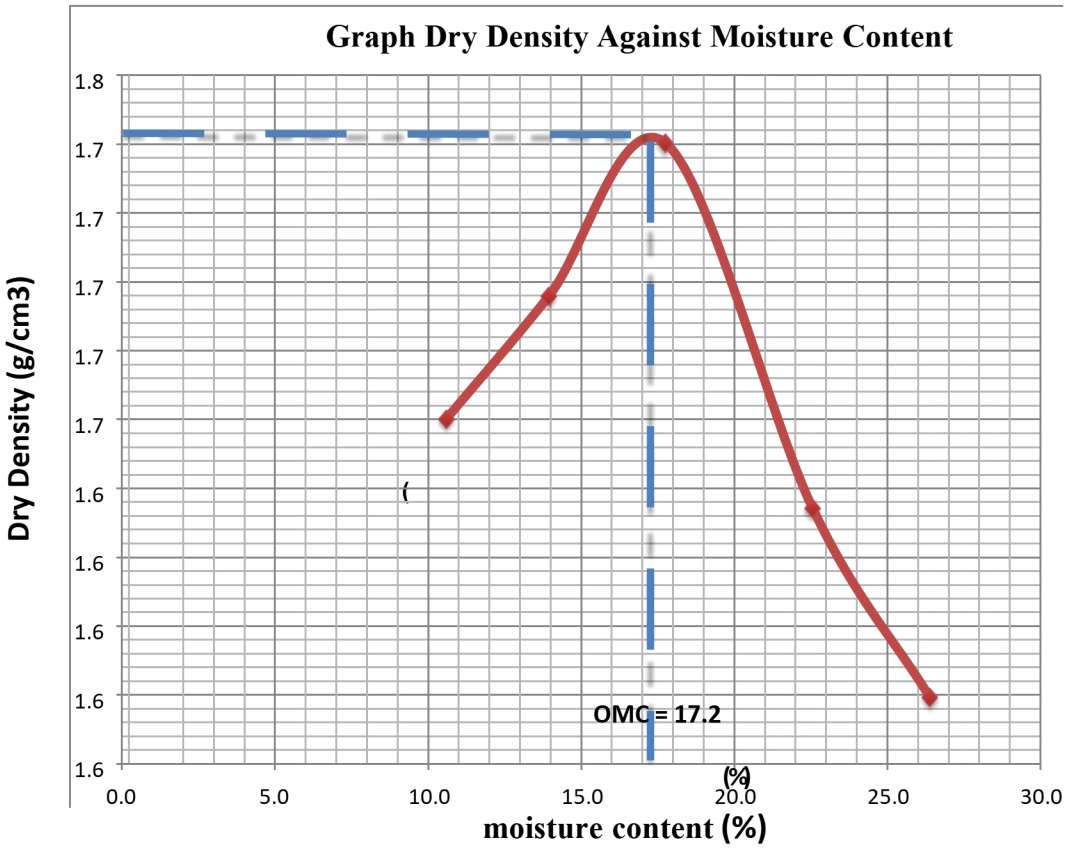

Table E3: Compaction characteristics of clay soil at depth 1.5m

TEST DATA										
Mold No.	OB		ABX		YA		17			
Wt. Wet Sample + Mold	5478		5570		5682		5640		5635	
Wt. of Mold	3703		3703		3703		3703		3703	
Wt. of wet Sample	1775		1867		1979		1937		1932	
Volume of sample	944		944		944		944		944	
Wet Density	1.88		1.98		2.10		2.05		2.05	
Cont.No.	1	2	3	4	5	6	7	8	9	10
Wt. Wet Sample + Cont	64.00	45.00	60.20	55.10	67.30	63.90	73.10	77.70	81.00	63.00
Wt. Dry Sample + Cont.	61.50	43.10	57.50	53.00	62.30	60.20	66.80	70.50	72.20	57.30
Wt. Water	2.50	1.90	2.70	2.10	5.00	3.70	6.30	7.20	8.80	5.70
Wt. Cont.	38.60	24.60	38.30	37.80	35.20	38.50	38.40	39.10	39.30	35.40
Wt, Dry Sample	22.9	18.5	19.2	15.2	27.1	21.7	28.4	31.4	32.9	21.9
Moisture Content %	10.9	10.3	14.1	13.8	18.5	17.1	22.2	22.9	26.7	26.0
Average moisture content %	10.59		13.94		17.75		22.56		26.39	
Dry Density	1.70		1.74		1.78		1.67		1.62	

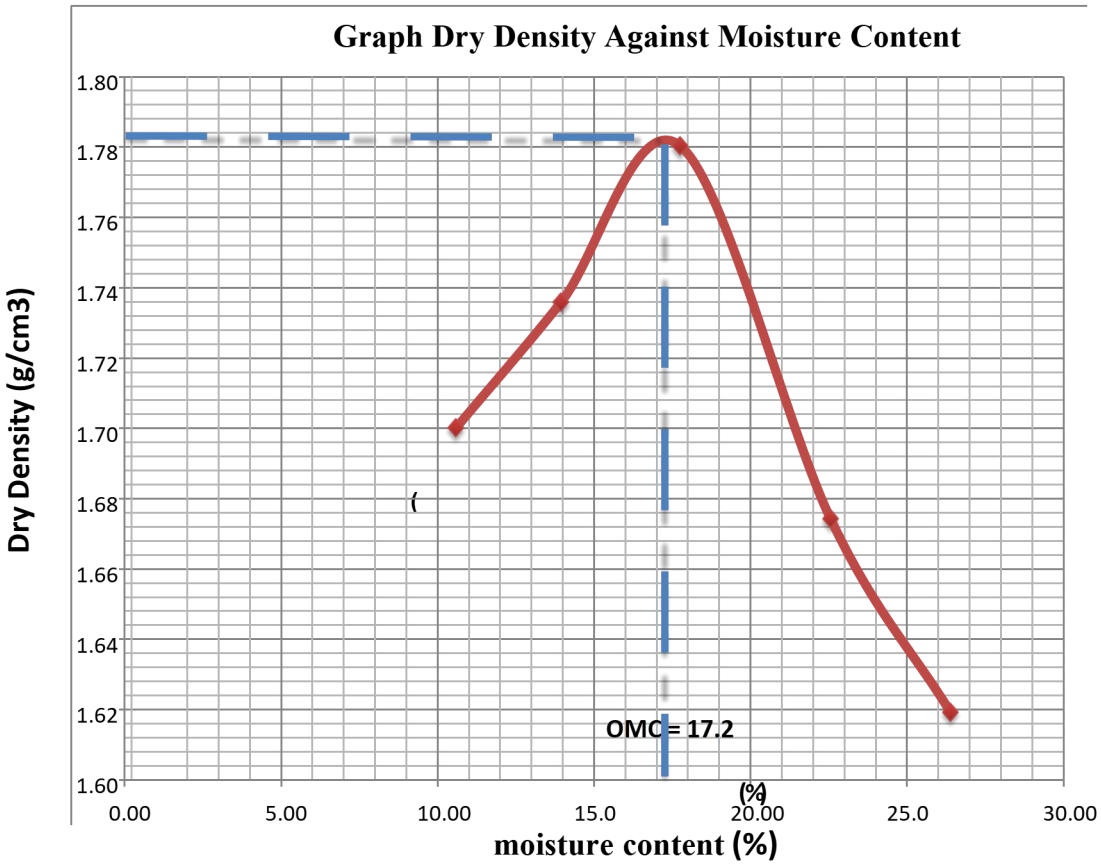
Graph Dry Density Against Moisture Content
Dry Density (g/cm3)
1.80
1.78
1.76
1.74
1.72
1.70
1.68
1.66
1.64
1.62
1.60
OMC = 17.2
0.00
5.00
10.00
15.0
20.00
25.0
30.00
moisture content (%)

Appendix F: Free Swell Index of Soil Samples

Table F1: Free Swell Index of test of clay soil at depth 0m

Trial	Vd(ml)	Vk(ml)	FSI (%)	Average FSI (%)
1	22.50	11.00	104.55	105.93
2	24.00	11.50	108.70	
3	22.50	11.00	104.55	

Table F2: Free Swell Index of test of clay soil at depth 1.0m

Trial	Vd(ml)	Vk(ml)	FSI (%)	Average FSI (%)
1	22.50	10.50	114.29	110.82
2	23.00	11.00	109.09	
3	23.00	11.00	109.09	

Table F3: Free Swell Index of test of clay soil at depth 1.5m

Trial	Vd(ml)	Vk(ml)	FSI (%)	Average FSI (%)
1	22.00	10.00	120.00	118.17
2	22.00	10.50	109.52	
3	22.50	10.00	125.00	